SGP-TR-124

COMPARISON OF PRESSURE TRANSIENT RESPONSE IN INTENSELY AND SPARSELY FRACTURED RESERVOIRS

Russell T. Johns

April 1989

I certify that I have read this report and that in my opinion it is fully adequate, in scope and in quality, as partial fulfillment of the degree of Master of Science in Petroleum Engineering.

Younes Jalali-Yazdi

Younes Jalali-Yazdi
(Principal advisor)

DISCLAIMER

DISTRIBUTION OF THIS DOCUMENT IS UNLIMITED

ii

Acknowledgments

I would like to thank my advisor, Dr. Younes Jalali-Yazdi, for spending a significant amount of time in giving invaluable advice and assistance in my research.

I am also grateful for the funding provided by the Geothermal Research Group of Stanford and the Chevron Corporation, which allowed me this opportunity.

Abstract

A comprehensive analytical model is presented to study the pressure transient behavior of a naturally fractured reservoir with a continuous matrix block size distribution. Geologically realistic probability density functions of matrix block size are used to represent reservoirs of varying fracture intensity and uniformity. Transient interporosity flow is assumed and interporosity skin is incorporated.

Drawdown and interference pressure transient tests are investigated. The results show distinctions in the pressure response from intensely and sparsely fractured reservoirs in the absence of interporosity skin. Also, uniformly and nonuniformly fractured reservoirs exhibit distinct responses, irrespective of the degree of fracture intensity. The pressure response in a nonuniformly fractured reservoir with large block size variability, approaches a nonfractured (homogeneous) reservoir response. Type curves are developed to estimate matrix block size variability and the degree of fracture intensity from drawdown and interference well tests.

Contents

List of Tables

List of Figures

Section 1

Introduction

It has long been recognized that naturally fractured reservoirs contain a significant portion of the world's hydrocarbon reserves. As such, the need to understand the detailed mechanisms of flow in these reservoirs is paramount. One of the main parameters that governs flow in fractured reservoirs is the matrix block size distribution. In one phase flow, it controls the transition from early production from the fractures to late production from the total reservoir (matrix and fractures). In two phase flow, it controls the rate of imbibition (or displacement) and ultimately the recovery efficiency of the reservoir [34].

Pressure transient testing provides a method to predict producibility in naturally fractured reservoirs. In order to estimate producibility, however, many assumptions are made. Certain assumptions, such as the idealization of a single matrix block size representing the reservoir, may be eliminated. Matrix block size distributions can be included in the model to more accurately describe the flow in naturally fractured reservoirs. The model presented in this study captures the intimacies of flow in a naturally fractured reservoir without complicating the task of analysis. The following are the key assumptions used in deriving the analytical solution:

- The primary porosity (matrix) is uniform, homogeneous and isotropic. The matrix blocks are defined by a characteristic length (volume of matrix block/surface area of matrix block, i.e. reciprical of specific surface area)

and are represented as slabs or plates. All matrix blocks have the same connectivity path to the wellbore.

- The secondary porosity (fractures) is uniform, homogeneous and isotropic.

- Flow occurs from the matrix into the fractures and then radially to the wellbore. No flow from the matrix to the wellbore is allowed and all flow is unsteady state (USS).

- The overall reservoir is infinite in extent and horizontal.

- The surface flow rate in the active well is constant, gravity effects are negligible, and Darcy's law is obeyed.

- A single phase fluid of small compressibility and constant viscosity flows through the medium.

In this report, a continuous probability density function of matrix block size is used. The interaction between the matrix and the fractures are defined by the following five parameters:

- h_{ratio}: the ratio of the characteristic lengths of the minimum and maximum matrix block size (h_{min}/h_{max}),

- w_m: the fractional storativity of the matrix,

- λ_{min}: the minimum interporosity flow coefficient which corresponds to the largest matrix block size,

- S_{ID}: the interporosity skin, and

- P(h): the probability density function describing the type of distribution of matrix block sizes.

Other parameters such as λ_{max}, the smallest matrix block interporosity flow coefficient, or w_f, the fractional storativity of the fractures, are determined from the parameters defined above. The only a priori knowledge needed in the analysis

is the type of distribution (i.e. exponentially decaying, exponentially increasing, linearly decreasing, linearly increasing, rectangular, or Dirac delta). The limits of the probability density function (i.e. h_{min} and h_{max}), however, do not need to be known and are obtained from the analysis of the pressure transient data.

Section 2

Literature Review

2.1 Geological Aspects

In order to analyze naturally fractured reservoirs, petroleum engineers have idealized complex fracture patterns into very simple geometric shapes. Without such simplification, the mathematical problem would be unsolvable. The idealized assumptions, however, are not as unrealistic as they may seem because fractures are created in a structured way. The orientations and distributions of fractures have been shown to be related to tectonic stresses and variations in these are due to local complexities of stress fields, rate of bending of the rocks, lithology and the proximity to fault planes.

According to Aguilera [2], fracture generation is generally attributed to three main causes:

- folding and faulting,

- deep erosion of the overburden that permits the upper parts to expand, uplift, and fracture through planes of weakness, and

- volume shrinkage (i.e. shales that lose water, cooling of igneous rocks, and desiccation of sedimentary rocks).

He also indicates that fractures and joints were usually formed in brittle rocks (especially those that are close to a fault plane). For instance, quartzite rocks have

a greater tendency to fracture than soft rocks such as limestones, which have a tendency to flow or bend.

Outcrops provide the best visual identification of the types of fracture patterns that exist. Dyer [22] presented spectacular aerial photographs of jointing of sandstones in the Arches National Park. The photographs clearly showed parallel fractures extending over a large distance. The joints were continuous in one direction but the majority did not link up in the perpendicular direction, and they were distributed in length such that there were more smaller joints than larger joints (i.e. exponential decaying or linearly decreasing). In terms of model simplification, these fractures can be represented as vertical or horizontal slabs. Other outcrops shown by Dyer, demonstrated the same type of parallel fractures, but with a subparallel set of fractures which were perpendicular to the top and bottom bedding surfaces. These fractures can be represented as either skewed rectangles, perpendicular rectangles or squares depending on the intersection angle of the fractures (Figure 2.1). In three dimensions, these can be modeled as cubes or rectangular parallelepipeds. Other fracture photographs show calcite cemented or mineral filled fractures that could restrict flow from one matrix block to another. This phenomenon is termed interporosity skin [14,38].

Pollard and Aydin [43] showed that most joints were not individually continuous but were usually a series of subparallel fractures (i.e. several smaller joints make up a larger joint). The spacing between the joints in sedimentary rocks generally had a regular distribution and were scaled with the thickness of the fractured layer. The outcrops studied suggested most joints (in sedimentary rocks) were perpendicular to the layering and were roughly rectangular in pattern. They also pointed out that joints rarely exceeded several hundred meters and were at least as long as several times the characteristic grain size of the rock. Fractures smaller than this were considered to be micro-cracks. Pollard and Aydin divided joint intersection geometries into orthogonal and nonorthogonal classifications. Either of these two classifications can be divided into three additional groups: continuous, continuous and discontinuous, and discontinuous. Depending on the combinations of these groups, '+', 'X', 'T', and 'Y' intersections can be formed (Figure 2.1). The greater the joint spacing

the greater the communication or linking between joints. Other joint types, such as echelon fractures can also be seen and are a result of the interaction of the stress relief caused by neighboring fractures.

Fractures in the Mt. Abott quadrangle of the central Sierra Nevadas were studied by Segall [46]. He discussed why fractures propagate and stop. Fractures grow when the extension force reaches a critical value (a property of the rock and environmental stress conditions) and stops due to elastic interaction from nearby cracks and an overall decrease in the systems effective stiffness. Again, the fracture (or fault) patterns were commonly arranged as echelon arrays. Many of these fractures were discontinuous and appeared to be randomly placed. This pattern can be modelled by a Monte Carlo approach or by using an infinite periodic array of cracks. In general, the fractures were parallel to each other, and the distribution in fracture lengths appeared to be exponential (i.e. there were many more smaller joints than larger joints). He also showed that joint lengths were comparable to lengths in the vertical exposure (i.e. these relationships exist in three dimensions).

McQuillan [37] described similar simple geometric fracture patterns (i.e. cubes or solid rectangles) in the Asmari formation of Southwestern Iran. In this formation, the fracture density (i.e. fracture length or matrix block size characteristic length) had an inverse logarithmic relation to bed thickness and was independent of structural setting.

Outcrops from the Monterey formation were examined by Isaacs [25]. She observed that fracture intensity was higher in thin beds than in the thick-bedded lower portion of the Monterey. Fracture intensity was generally higher in quartzite bearing rocks than in other lithology types such as opal-CT bearing rocks.

Reiss [44] also used simple geometric shapes to represent fracture systems. He used four principal representations: sheets or slabs, match-sticks, cubes, and cubes with an impermeable fracture plane. The impermeable fracture plane could be due to mineral precipitation. He added complexity to these shapes by considering the flow to be either vertical or horizontal to the faces. He presented relationships between fracture permeability, porosity, width, and matrix size for these various simplified geometries.
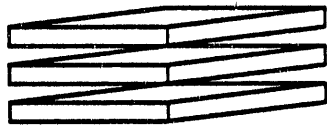
Slabs
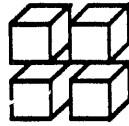
Cubes
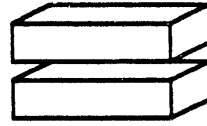
Rectangular
Parallelepipeds
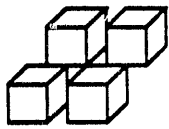
Skewed Cubes
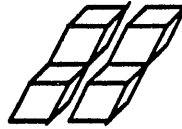
Rhombuses

Skewed
Rectangular
Parallelepipeds

Rhombohedral
Rectangular
Parallelepipeds

Random Fractures
or Joints
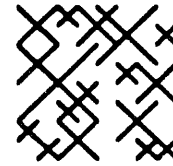
Bi-Directional
Random Fractures
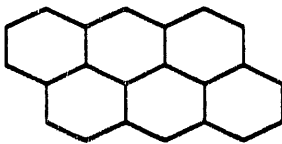
Polygonal
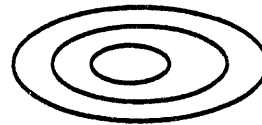
Eliptical

Figure 2.1: Idealizations of Typical Fracture Patterns seen in Nature.

2.2 Well Testing Aspects

Barenblatt *et al.* [4,5] introduced the concept of a double porosity system for naturally fractured reservoirs. The concept implies that, at every point in the reservoir, there are two fluid pressures; one in the fracture and one in the matrix. Flow equations from the matrix to the fracture were linked using the assumption of pseudo steady state (PSS), which related the flow rate from the matrix to the fracture to the difference between the matrix pressure and the fracture pressure (i.e. explicitly independent of time). Flow from the fracture to the wellbore was assumed to be unsteady state.

The relationship between recovery behavior for a single reservoir matrix block and its size was defined by Mattax and Kyte [34]. It was qualitatively shown that the recovery efficiency due to imbibition was proportional to the square of the distance between fractures. The paper defined the critical water injection rates necessary to adequately sweep hydrocarbons from a matrix block. [1]

Warren and Root [52] presented essentially the same model as Barenblatt *et al.*, but defined the problem in terms of petroleum engineering variables. They presented a model of an orthogonal system of continuous uniform fractures, but in fact did not use the specified geometry. They introduced λ, the interporosity flow coefficient, and ω, the fractional storativity of the fractures. Using λ and ω they characterized the pressure transient response expected from buildup and drawdown well tests. Two parallel lines were shown to exist in a semilog plot of pressure versus time. A transition from fracture flow to fracture and matrix flow connected the two parallel straight lines. They showed that as ω or λ approaches one, the reservoir transient test behaved like that of a homogenous reservoir. The interporosity flow coefficient λ contained the geometry dependent parameter α, but this parameter was not directly included in their work.

Some well tests, however, did not show parallel straight lines. Odeh [41] gave examples of well tests from fractured reservoirs that did not exhibit the double

---

[1] They considered scaling parameters in an imbibition displacement. This was not a paper on well testing for fractured reservoirs.

porosity behavior. He suggested the double porosity behavior cannot be seen because reliable data are not obtained during the early part of well tests (i.e. storage effects). Essentially, Odeh translated the anisotropic model of Warren and Root to an isotropic one.

Several years later, Kazemi *et al.* [32] extended Warren and Root's double porosity model to interference well tests. Kazemi considered an infinite reservoir with a constant rate of production at the observation well. Like others, Kazemi incorporated PSS flow from the matrix to the fractures. The solution was solved in Laplace space and was numerically inverted. Some important conclusions were that the double porosity model was important for early pressure transient responses, and that at late times, the model approached the homogeneous finite well source solution. In the same year, Kazemi [31] presented additional work on pressure transient responses in reservoirs with uniform fracture distributions. This work dropped the assumption of PSS and used an unsteady state formulation of flow from the matrix to the fractures. The reservoir considered was two-dimensional, circular, and finite. They explored allowing the matrix fluid to flow into the wellbore directly, but they showed that this effect was insignificant for low matrix permeability. They concluded the USS formulation increased the length of the transition zone but did not alter the early and late time parallel straight lines.

In the mid-seventies, De Swaan [17] also used the assumption of USS interporosity flow. Approximate equations to early and late time responses were presented by the inclusion of a hydraulic diffusivity constant. De Swaan considered horizontal fractures and spherical matrix blocks.

Najurieta [39,40] solved the interference well test case using De Swaan's USS solution for both slab and cubic geometries (assuming an infinite reservoir). Najurieta used an improved Schapery [45] inversion technique to transform the solution from Laplace space to real time space. This improved the approximation of the early, transition, and late time responses.

Deruyck [20] considered interference well tests using Warren and Root's model. He considered both constant pressure and constant rate inner boundary conditions and applied the PSS interporosity flow assumption. Type curves were presented for

both constant pressure and constant rate inner boundary conditions. He compared the line source solution to the finite well radius solution and observed no significant differences for observation wells greater than approximately twenty feet from the active well. Most importantly, he introduced a new parameter Θ ($\Theta = \lambda r_d^2$) that eliminated the need for more than one type curve for constant rate production. He provided the theoretical basis for this new parameter from the approximate line source solution. Later, Deruyck *et al.* [21] presented essentially the same conclusions, but presented interference well test type curves for both USS and PSS interporosity flow assumptions. They suggested using the type curve that best fits the data. In addition, they concluded the double porosity effect can be better seen for observation wells closer to the active well.

The first useful type curves for buildup and drawdown tests were prepared by Bourdet and Cringarten [10]. The type curves used PSS and USS interporosity flow assumptions but were based on approximations of the exact solutions.

Unsteady state interporosity flow for both cylindrical and spherical geometries was considered by Kuchuk and Sawyer [33]. They concluded the Warren and Root model was only applicable under special cases of the fractured reservoir parameters.

Cinco-Ley and Samaniego [13] also used the USS formulation proposed by De Swaan using spheres and slab matrix block geometries. At early and late times, the pressure transient responses were similar. During the transition phase, however, differences were seen between the two geometries. In a later paper, Cinco-Ley *et al.* [14] described the effects of multiple matrix block sizes on the pressure transient curve. They used a discrete model of up to five different block sizes. Using combinations of these block sizes, they demonstrated the transition zone was affected significantly, while the late and early time responses were not changed. They state the smaller matrix block sizes dominated the transition period since the surface to fracture contact area was greater. In addition, both Cinco-Ley *et al.* and Moench [38] presented an explanation for the observance of the PSS behavior. They introduced an interporosity skin factor that, in conjunction with USS interporosity flow assumptions, produced the PSS-like behavior.

Streltsova [50] explored the differences between the USS and PSS flow models.

She showed that small matrix blocks have a pressure response more like the PSS behavior, while larger matrix blocks behaved more like USS. The larger the matrix blocks, therefore, the longer the transition zone.

The PSS and USS solutions were combined into one model by Jalali-Yazdi and Ershaghi [28]. Their solution used the Najurieta approximation (improved Schapery approximation) to develop functions of time that describe the interporosity flow interaction. Also, they presented a correlation for parameter estimation, using the difference between the wellbore pressure response and either the early time or the late time pressure response.

Braester [11] presented numerical solutions which showed that drawdown pressures were not sensitive enough to the variation in sizes of the blocks (especially for matrix blocks not in the immediate vicinity of the wellbore). She suggested, therefore, that drawdown and buildup well tests do not yield a unique solution for matrix block sizes.

In a recent paper, Belani and Jalali-Yazdi [7] extended the discrete model proposed by Cinco-Ley and Samaniego [13] to a continuous model (i.e. a continuous probability density function of matrix block sizes). They used three probability density functions: Dirac delta, uniform and bimodal. The Dirac delta function resulted in a sharp pressure response identical to the Warren and Root model. With an increase in the variance of the matrix block size distribution, they found features of a fractured reservoir response become less pronounced.

Section 3

Statement of the Problem

Currently, block size distribution is not considered a determinable parameter from well pressure transient testing. Yet, the utility of determining the matrix block size distribution is paramount since block size is considered one of the main parameters of a fractured reservoir [11]. In single phase flow, it controls the transition from early production of hydrocarbons from the fractures to late production from the total reservoir. In reservoirs with two-phase flow, it controls the rate of imbibition (or displacement) and ultimately the recovery efficiency of the reservoir (i.e. waterflood injection rate).

The objective of this research is to infer fracture intensity and the degree of fracture uniformity from transient pressure data. It is recognized that this can only be done in a qualitative way for many reservoirs. Nevertheless, a completely quantitative solution based on some specified assumptions (i.e. slab matrix block geometry) is presented. Certainly, this research can be modified for the particular constraints of any given reservoir. Other information, such as that from cores and logs, should be used in conjunction with well pressure testing, to evaluate the distribution of fractures.

Section 4

Theory and Solution

4.1 General Solution

The diffusivity equation for a double porosity reservoir can be modified to include a probability distribution of matrix block size by introducing a source integral [7]:

$$\frac{k_f}{\mu} \nabla^2 P_f = \phi_f c_f \frac{\partial P_f}{\partial t} + \int_{h_{min}}^{h_{max}} Q(h) P(h) \, dh \,. \tag{4.1}$$

The source integral in Equation 4.1 accounts for the flow contribution of the matrix to the fracture. It is assumed that fluid travels from the matrix to the fractures and to the wellbore. P(h) is the probability density function (PDF) describing the likelihood of a certain matrix block size to exist and Q(h) is the flow contribution from that matrix block to the fracture. For transient interporosity flow and slab geometry:

$$Q(h) = -\frac{k_m}{\mu h} \nabla p_m \big|_{interface} \,. \tag{4.2}$$

Q(h), therefore, takes into consideration the mode of interporosity flow and also the geometry of the matrix blocks.

For a well producing at constant rate in an infinite reservoir, the interference solution in Laplace space is:

$$\overline{P}_{D_f} = \frac{K_0(x r_D)}{s[C_D s(K_0(x) + S_D x K_1(x)) + x K_1(x)]} \,, \tag{4.3}$$

13

and for drawdown:

$$\overline{P}_{D_w} = \frac{K_0(x) + S_D x K_1(x)}{s[C_D s(K_0(x) + S_D x K_1(x)) + x K_1(x)]}. \tag{4.4}$$

Parameter s is the Laplace variable related to dimensionless time (t_D) and the Bessel function argument is:

$$x = \sqrt{sf(s)}. \tag{4.5}$$

The function f(s) embodies the reservoir parameters including the matrix block size distribution. For transient interporosity flow in the presence of interporosity skin:

$$f(s) = \omega_f + \omega_m \int_{h_{ratio}}^1 \frac{\sqrt{\frac{\lambda}{\omega_m s}}\tanh(\sqrt{\frac{\omega_m s}{\lambda}})P(h_D)}{1 + S_{ID}\sqrt{\frac{\omega_m s}{\lambda}}tanh(\sqrt{\frac{\omega_m s}{\lambda}})} dh_D, \tag{4.6}$$

where,

$$h_{ratio} = \frac{h_{min}}{h_{max}}, \tag{4.7}$$

$$S_{ID} = \frac{k_m h_s}{k_s h}. \tag{4.8}$$

The interporosity skin factor (S_{ID}) is a function of matrix block size distribution and, hence is constant if $\frac{h_s}{h}$ is constant. An alternate assumption is that the depth of skin damage (h_s) is constant for all matrix blocks, and hence, S_{ID} is a variable:

$$S_{ID} = S_{IDmin}\sqrt{\frac{\lambda}{\lambda_{min}}}, \tag{4.9}$$

where,

$$S_{IDmin} = \frac{k_m h_s}{k_s h_{max}}, \tag{4.10}$$

and now:

$$f(s) = \omega_f + \omega_m \int_{h_{ratio}}^1 \frac{\sqrt{\frac{\lambda}{\omega_m s}}\tanh(\sqrt{\frac{\omega_m s}{\lambda}})P(h_D)}{1 + S_{IDmin}\sqrt{\frac{\omega_m s}{\lambda_{min}}}tanh(\sqrt{\frac{\omega_m s}{\lambda}})} dh_D. \tag{4.11}$$

4.2 Long Time Approximation

As t_D becomes large, the Laplace space variable s becomes small. As s approaches zero, the function f(s) becomes one. Neglecting wellbore storage and inverting to the time domain, Equation 4.4 yields:

$$P_{D_w} = \frac{1}{2}[ln(t_D) + 2S_D + .80907],\qquad(4.12)$$

and Equation 4.3 yields:

$$P_{D_f} = \frac{1}{2}[ln(\frac{t_D}{r_D^2}) + .80907].\qquad(4.13)$$

4.3 Early Time Approximation

As t_D becomes very small, the Laplace space variable s becomes large and the function f(s) approaches ω_f, the fractional storativity of the fractures. In the absence of wellbore storage and skin, inversions of Equation 4.4 give:

$$P_{D_w} = 2\sqrt{\frac{t_D}{\omega_f \pi}}.\qquad(4.14)$$

This early time solution should not be confused with the 'classical' early parallel straight line response given by:

$$P_{D_w} = \frac{1}{2}[ln(\frac{t_D}{\omega_f}) + 2S_D + .80907].\qquad(4.15)$$

Section 5

Probability Density Functions

Prediction of the pressure response requires the type of matrix block size distribution be known or assumed. When the PDF is selected, fracture intensity can be inferred from pressure transient data. Two types of probability density functions are used to represent the variability of matrix block size. These types, exponential and linear (Figure 5.1), occur in outcrops as indicated in the geological literature [22,43,46]. The Dirac delta and rectangular distribution are each subsets of the exponential and linear distributions.

The mean of a distribution is a measure of fracture intensity, while the variance is a measure of the degree of fracture uniformity. As fracture intensity increases, mean block size decreases and P(h) becomes skewed toward smaller block sizes. As fracture intensity decreases, P(h) becomes skewed toward large block sizes. When fracturing becomes uniform, h_{ratio} approaches unity and P(h) becomes 'narrow'. When fracturing becomes nonuniform, h_{ratio} approaches zero and P(h) becomes 'wide'.

Figure 5.2 is an example of the construction of a probability density function [3]. The lengths of the joints were measured at the outcrop and plotted as shown. There are many more smaller joints than larger joints. In this example, h_{min} is one meter and h_{max} is approximately thirty-three meters. The parameter h_{ratio}, therefore, is small (.03) indicating very nonuniform fracturing. A probability density function is then constructed by normalizing the frequency plot by the parameter h_{max}. The

result is a normalized probability density function that is exponentially decaying with a decay constant ('a') of -5.

5.1 Exponential and Linear PDF

The exponential PDF is given by:

$$P(h_D) = \frac{a(exp^{-ah_D})}{exp^{-(ah_{ratio})} - exp^{-a}}, \tag{5.1}$$

where 'a' is the exponential constant. The linear distribution function is:

$$P(h_D) = \frac{mh_D + b}{.5m(1 - h_{ratio}^2) + b(1 - h_{ratio})}, \tag{5.2}$$

where 'm' is the slope and 'b' is the vertical intercept of the cartesian plot of $P(h_D)$ versus h_D. Because a probability function must be positive, the slope must be in the range:

$$\frac{-2}{(1 - h_{ratio})^2} \leq m \leq \frac{2}{(1 - h_{ratio})^2}. \tag{5.3}$$

The intercept 'b' is given by:

$$b = \frac{1 - .5m + .5h_{ratio}^2}{1 - h_{ratio}}. \tag{5.4}$$

5.2 Limiting Forms-Rectangular and Dirac Delta Distributions

When 'm' is zero (linear PDF) or 'a' is zero (exponential PDF), both probability density functions reduce to the rectangular distribution:

$$P(h_D) = \frac{1}{1 - h_{ratio}}, \tag{5.5}$$

and when 'm' or 'a' approach infinity, the distributions reduce to the Dirac delta function:

$$P(h_D) = \delta(h_D - 1) = \begin{cases} 0 & \text{for } h_D \neq 1 \\ \infty & \text{for } h_D = 1 \end{cases}. \tag{5.6}$$
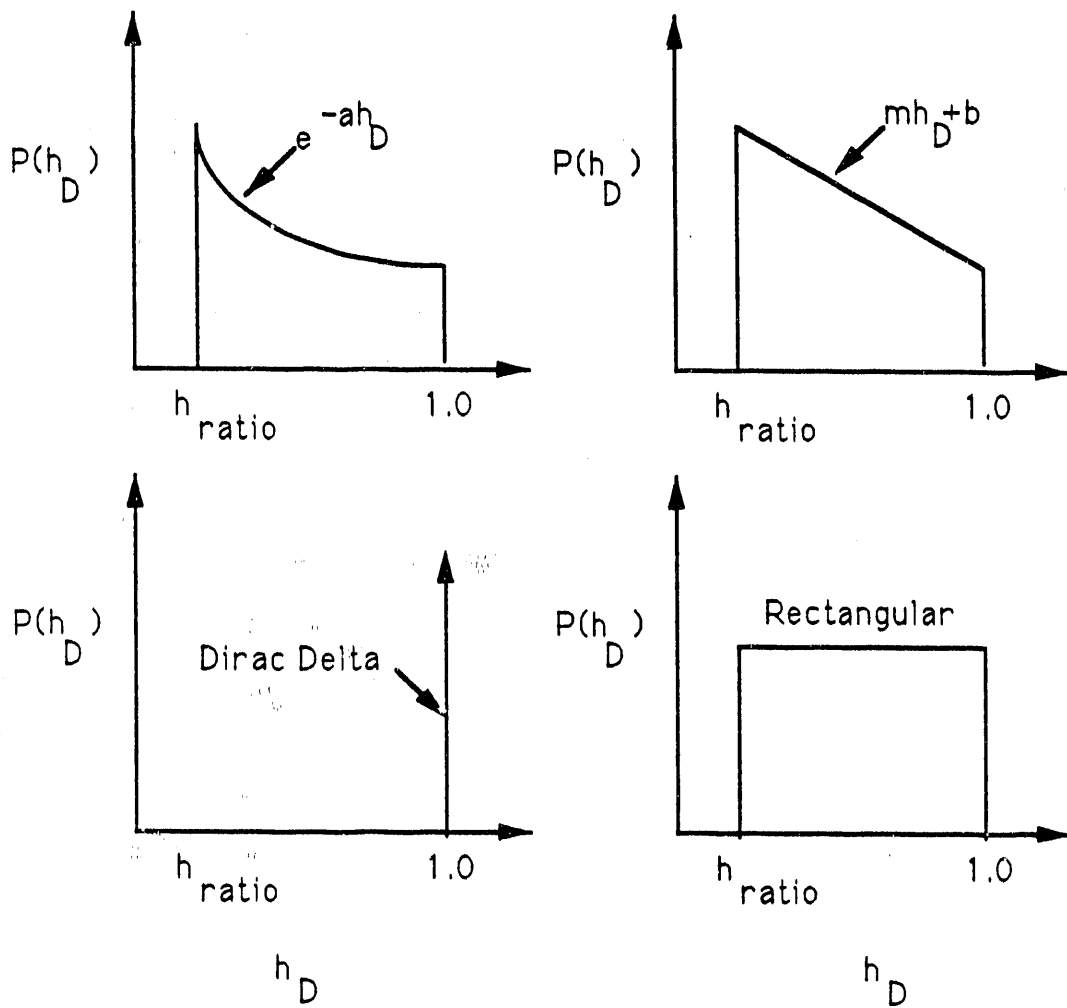
Figure 5.1: Probability Density Functions.
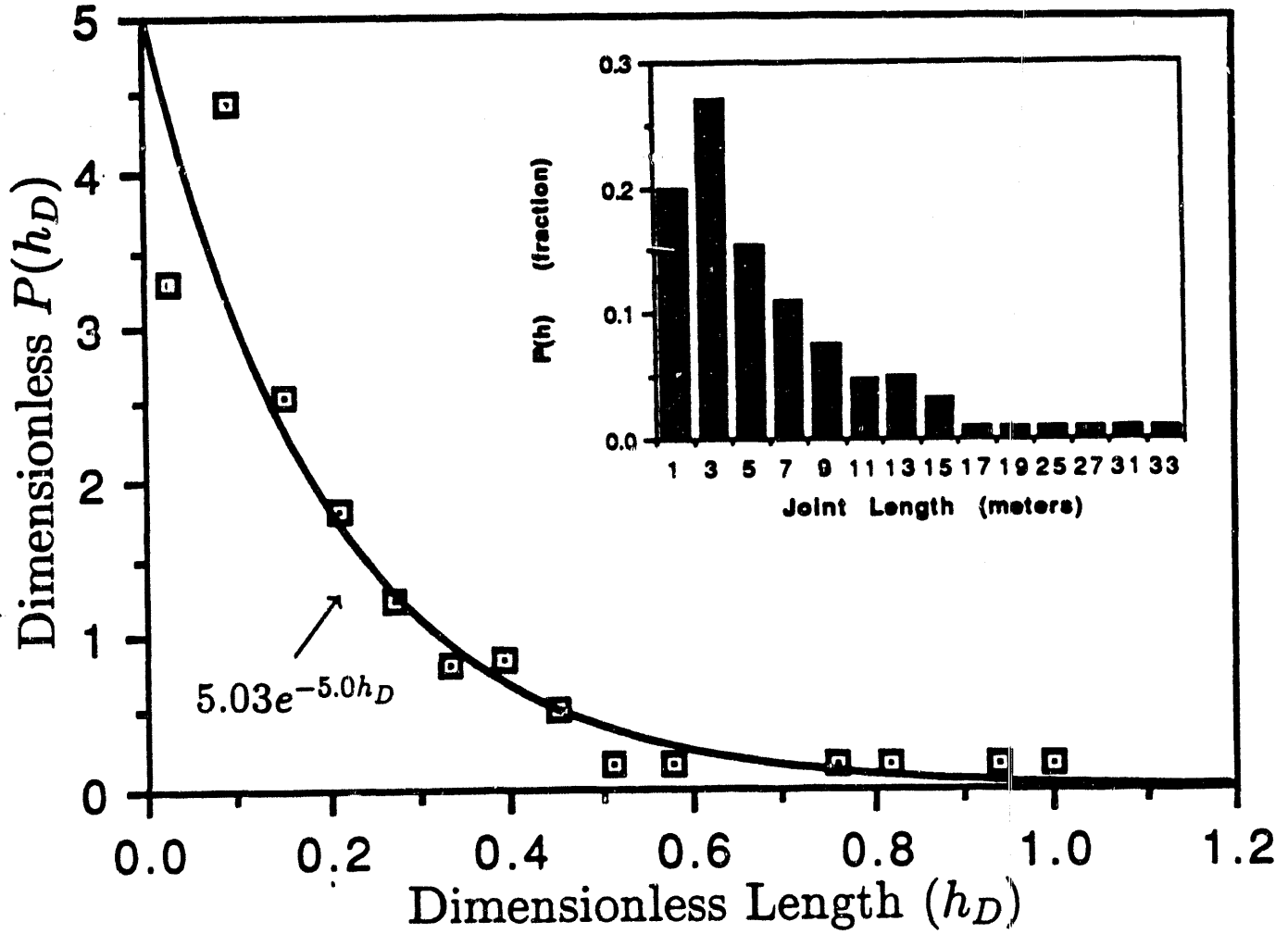
Figure 5.2: Construction of Probability Density Function from Outcrop, Central Sierra Nevadas.

PDF	$f(s)$, where $\xi = \sqrt{\frac{\omega_m s}{\lambda_{min}}}$
Exponential	$\omega_f + \dfrac{a\omega_m}{\xi(e^{-ah_{ratio}} - e^{-a})} \displaystyle\int_{\xi h_{ratio}}^{\xi} \dfrac{e^{\frac{-ay}{\xi}} tanh(y)}{y[1 + S_{ID_{min}} \xi \, tanh(y)]} dy$
Linear	$\omega_f + \dfrac{\omega_m}{\xi[.5m(1 - h_{ratio}^2) + b(1 - h_{ratio})]} \displaystyle\int_{\xi h_{ratio}}^{\xi} \dfrac{[\frac{m}{\xi} + \frac{b}{y}] tanh(y)}{1 + S_{ID_{min}} \xi \, tanh(y)} dy$
Rectangular	$\omega_f + \dfrac{\omega_m}{\xi(1 - h_{ratio})} \displaystyle\int_{\xi h_{ratio}}^{\xi} \dfrac{tanh(y)}{y[1 + S_{ID_{min}} \xi \, tanh(y)]} dy$
Dirac delta	$\omega_f + \dfrac{\omega_m tanh(\xi)}{\xi[1 + S_{ID} \xi tanh(\xi)]}$, where $\lambda_{min} = \lambda_{max} = \lambda$

Table 5.1: Functions f(s) for Various PDF's.

The Dirac delta distribution describes fractures that are perfectly ordered as in the Warren and Root model. The rectangular distribution, however, represents fractures that are perfectly disordered with a continuum of block sizes that are equally probable from the smallest (h_{min}) to the largest (h_{max}). In general, the rectangular distribution should be used if the distribution type is unknown.

Upon specifying the type of PDF, Equation 4.11 can be solved for f(s). Table 5.1 lists the solutions of f(s) for the particular PDF.

Section 6

Discussion-Drawdown Testing

Equation 4.4 in the absence of wellbore storage and skin reduces to:

$$\overline{P}_{D_w} = \frac{K_0(\sqrt{sf(s)})}{s^{3/2}\sqrt{f(s)}K_1(\sqrt{sf(s)})}. \qquad (6.1)$$

Equation 6.1 is numerically evaluated using the Stehfest algorithm [48] for the exponential PDF listed in Table 5.1. Figure 6.1 illustrates the response for varying values of 'a' holding h_{ratio} constant. For positively increasing values of 'a', fracture intensity increases and the response approaches the Dirac delta response for a uniform matrix block size h_{min} (i.e. the response occurs earlier in time). For negatively increasing values of 'a', fracture intensity decreases and the response approaches the Dirac delta response for a uniform matrix block size h_{max} (i.e. the response occurs later in time). Thus, fracture intensity determines the temporal position of the pressure response. Fracture uniformity, however, affects the shape of the pressure response. From Figure 6.1, it is evident the derivative profile shows a substantial degree of asymmetry with respect to the time axis as 'a' increases or decreases to large absolute values. The response for the rectangular matrix block size distribution (i.e. a=0), however, is nearly symmetric. Therefore, asymmetry increases as fracturing becomes more uniform, and the shape of the derivative profile can be used as a qualitative indicator of the degree of matrix block size variability or nonuniformity.

21
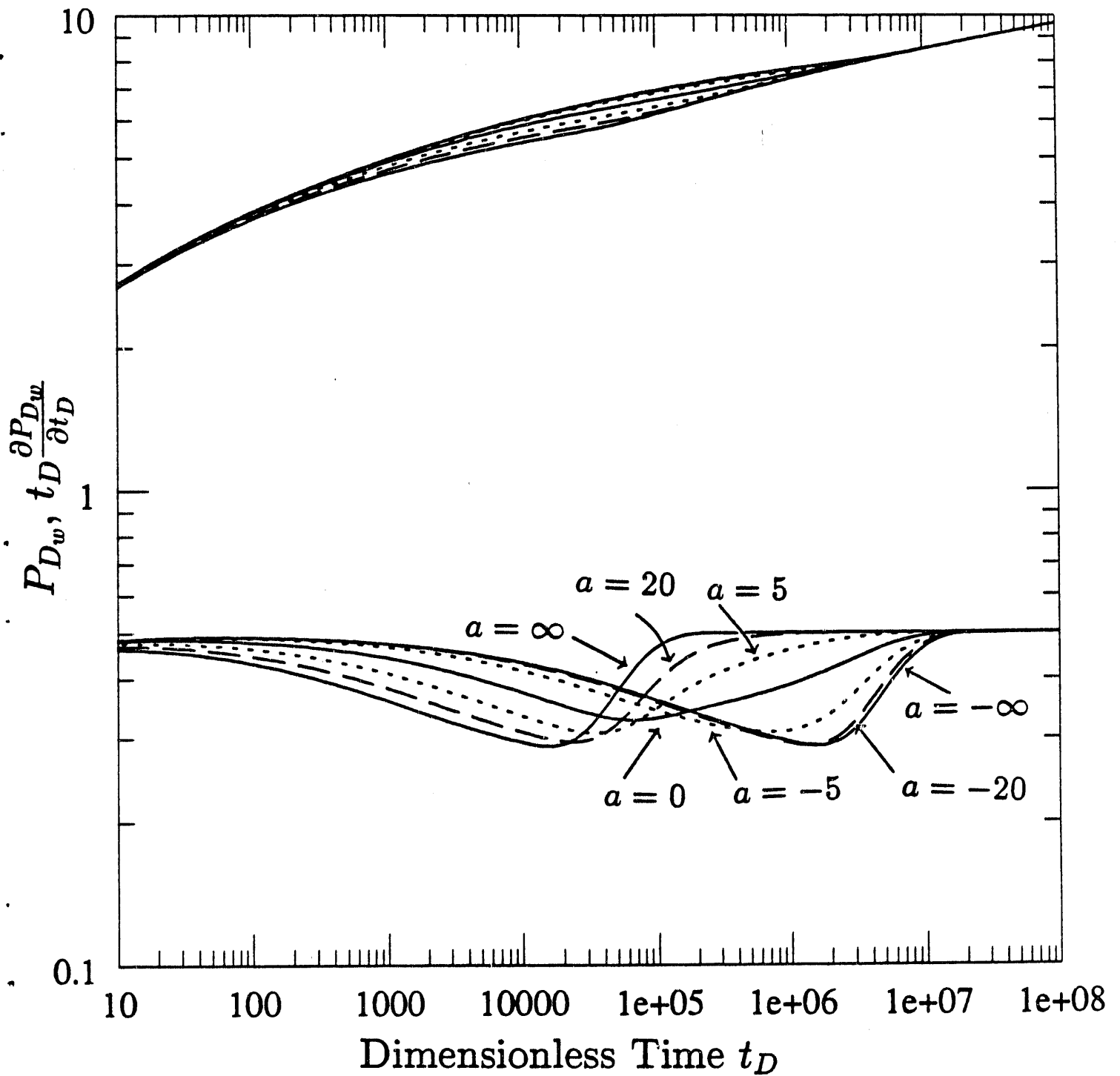
Figure 6.1: Exponential PDF: Varying 'a' with $h_{ratio} = .1$, $\lambda_{min} = 10^{-7}$, $\omega_m = .9$.

In addition, parameter h_{ratio} provides an estimate of matrix block size variability. An h_{ratio} approaching one indicates perfectly uniform fracturing, while h_{ratio} approaching zero indicates perfectly nonuniform fracturing. Figure 6.2 illustrates the pressure response for varying values of h_{ratio} with 'a' held constant. For h_{ratio} approaching zero, the response approaches a homogenous reservoir response. This occurs because there is an incessant gradual contribution from the matrix to the fractures. As long as fracturing is extremely nonuniform, the response will not exhibit the classical profile of a distinct transition zone separating early and late time semilog straight lines.

6.1 Type Curve For Drawdown Well Tests

For the rectangular PDF, a type curve can be developed for estimation of ω_m, λ_{min}, and h_{ratio}. The type curve is based on the following time domain solution of the wellbore pressure response:

$$P_{D_w} = \frac{1}{2}[ln(\frac{t_D}{F(t_D)r_D^2}) + .80907],$$ (6.2)

where $F(t_D)$ is the time-dependent reservoir storativity:

$$F(t_D) = \omega_f + \omega_m \int_{h_{ratio}}^{1} \sqrt{\frac{t_D}{\tau}} tanh(\sqrt{\frac{\tau}{t_D}})P(h_D)\,dh_D,$$ (6.3)

and τ is the matrix response time coefficient:

$$\tau = \frac{\omega_m}{\gamma\lambda}.$$ (6.4)

Equations 6.2 and 6.3 are obtained by applying the inversion technique of Najurieta and Schapery [45,40,39]. For the rectangular PDF, Equation 6.3 becomes:

$$F(\frac{t_D}{\tau_{max}}) = \omega_f + \frac{\omega_m}{(1 - h_{ratio})}\sqrt{\frac{t_D}{\tau_{max}}} \int_{h_{ratio}\sqrt{\frac{\tau_{max}}{t_D}}}^{\sqrt{\frac{\tau_{max}}{t_D}}} \frac{tanh(y)}{y}\,dy,$$ (6.5)

where y is the variable of integration and τ_{max} is the response time coefficient of the most dormant (or largest) matrix block:

$$\tau_{max} = \frac{\omega_m}{\gamma\lambda_{min}}.$$ (6.6)
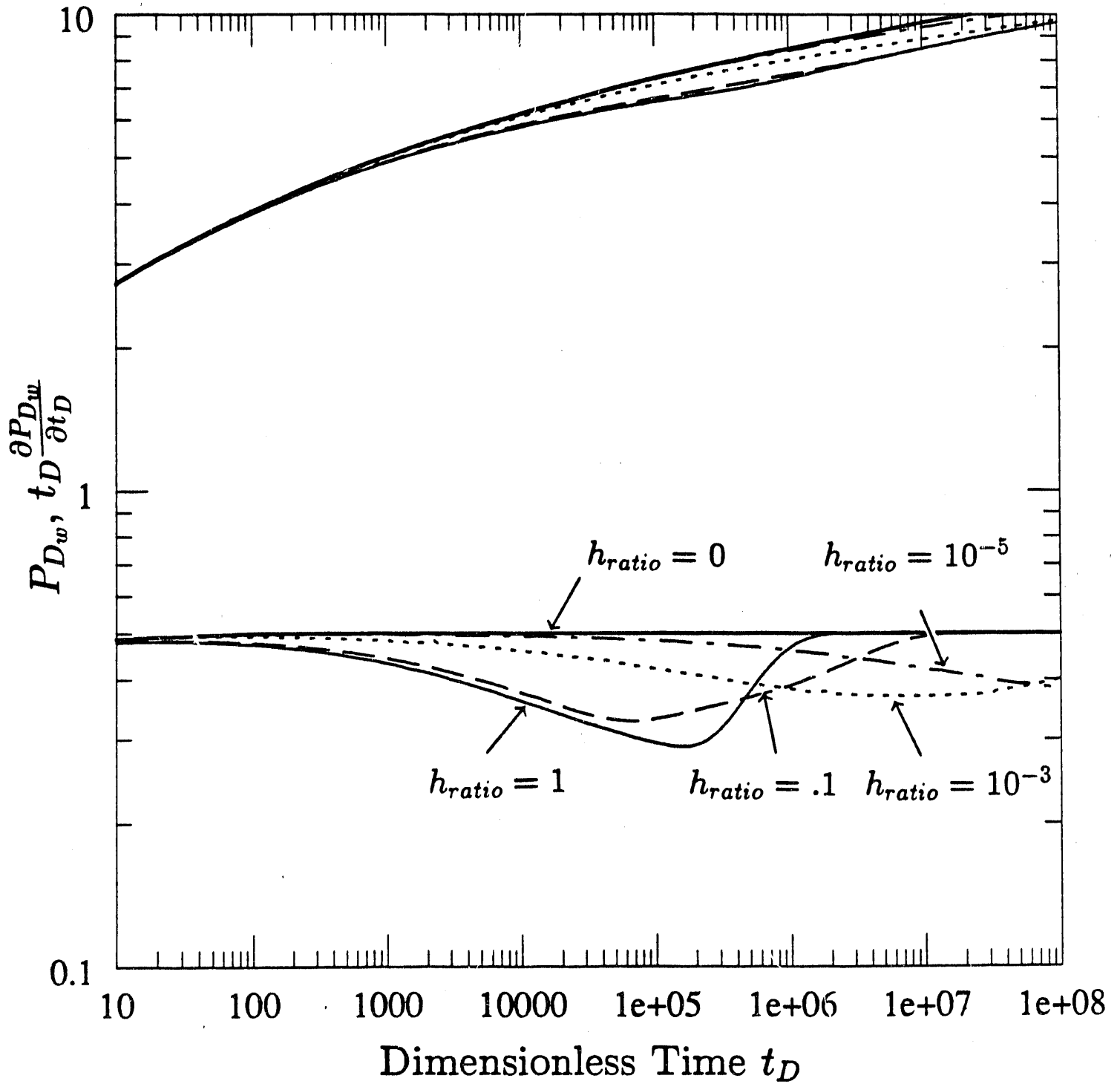
Figure 6.2: Rectangular PDF: Varying h_{ratio} for Geometric Mean $\lambda = 10^{-6}$, $\omega_m = .9$.

In general, the time domain approximation gives remarkably good results (Figure 6.3). Using the difference between the extrapolated late time pressure response and the observed pressure, one obtains:

$$\Delta P = P_{D_w} - P_{D_{w_{late}}} = -\frac{1}{2}lnF(\frac{t_D}{\tau_{max}}).$$
(6.7)

The type curve (Figure 6.4) is generated for the rectangular PDF by plotting the pressure difference ΔP versus $\frac{t_D}{\tau_{max}}$ for a range of h_{ratio} and ω_m values. This type curve is similar to one presented by Jalali-Yazdi and Ershaghi [27] where the time match yields τ_{max} (and hence, λ_{min}), and the pressure match yields ω_m. Fracture permeability, k_f, can be calculated from the slope of the semilog straight line. Given reliable estimates of matrix permeability (i.e. from core analysis), one can calculate h_{max} from the definition of λ_{min} given in Appendix A. From the shape of the curve, h_{ratio} is estimated, and hence, h_{min} is determined. The arithmetic mean of h_{min} and h_{max} is a measure of fracture intensity or sparsity.

The type curve demonstrates two key ideas. First, as matrix storativity predominates (increasing ω_m), h_{ratio} affects the pressure response more significantly. Conversely, as ω_m decreases, the effect of matrix block size variability becomes less significant. Second, the effect of h_{ratio} on the pressure response is greatest for lower values of h_{ratio} (e.g. the pressure response changes more significantly for h_{ratio} values from 0.1 to 0.5 than from 0.5 to 1.0). This indicates that block size variability affects the pressure response significantly if h_{min} and h_{max} differ by at least one order of magnitude. Block size variability less than half an order of magnitude does not affect the pressure response significantly.

6.2   Effect of Interporosity Skin

An example of the effect of interporosity skin ($S_{ID_{min}}$) on the pressure transient response is shown in Figure 6.5. A significant change in the pressure derivative is seen for small changes in $S_{ID_{min}}$, and thus, the effect of the matrix block size distribution is masked. The derivative profile becomes symmetric and more pronounced
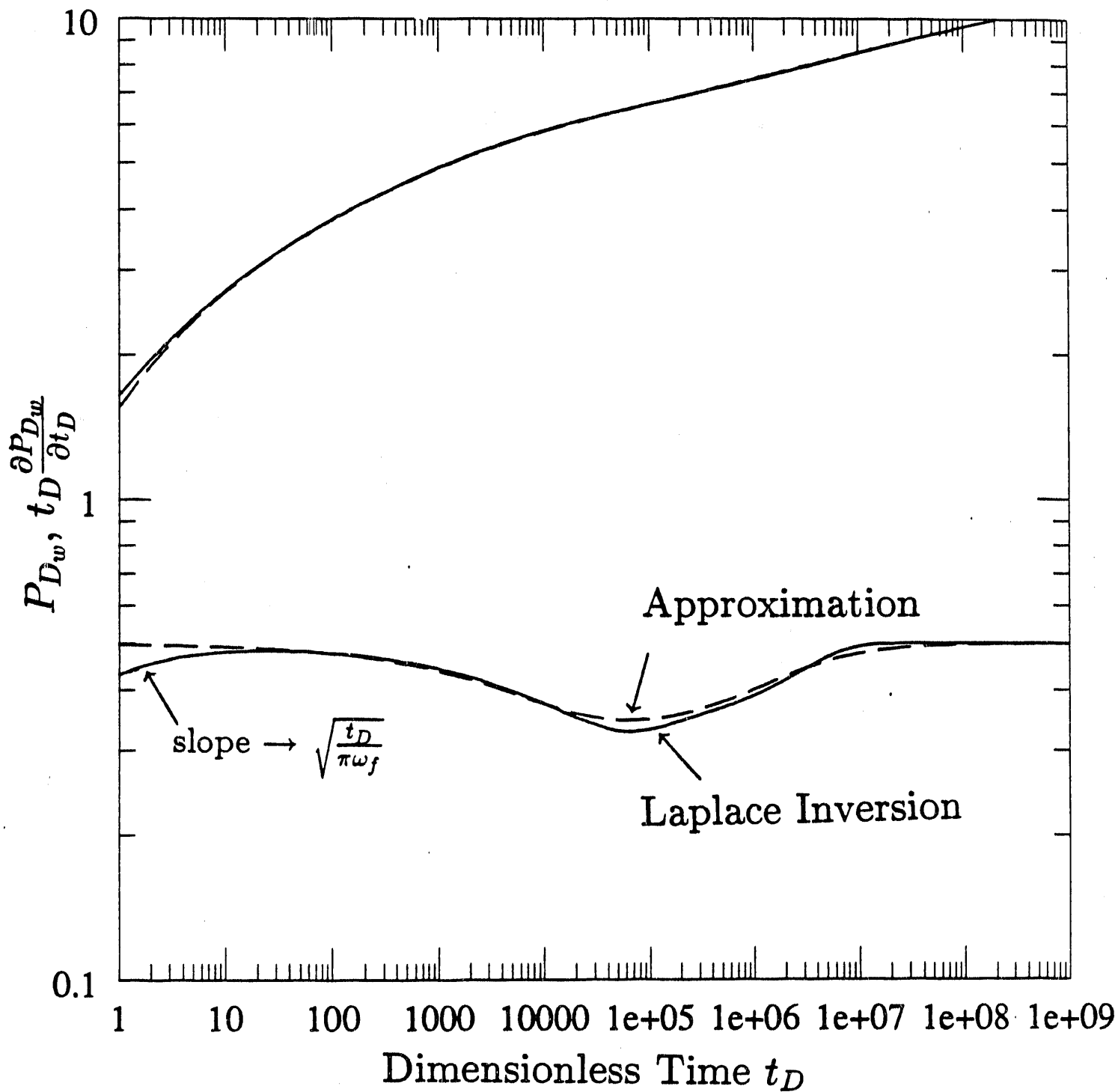
Figure 6.3: Rectangular PDF: Solution by Stehfest Inversion versus Time Domain Approximation, $h_{ratio} = .1$, $\lambda_{min} = 10^{-7}$, $\omega_m = .9$.
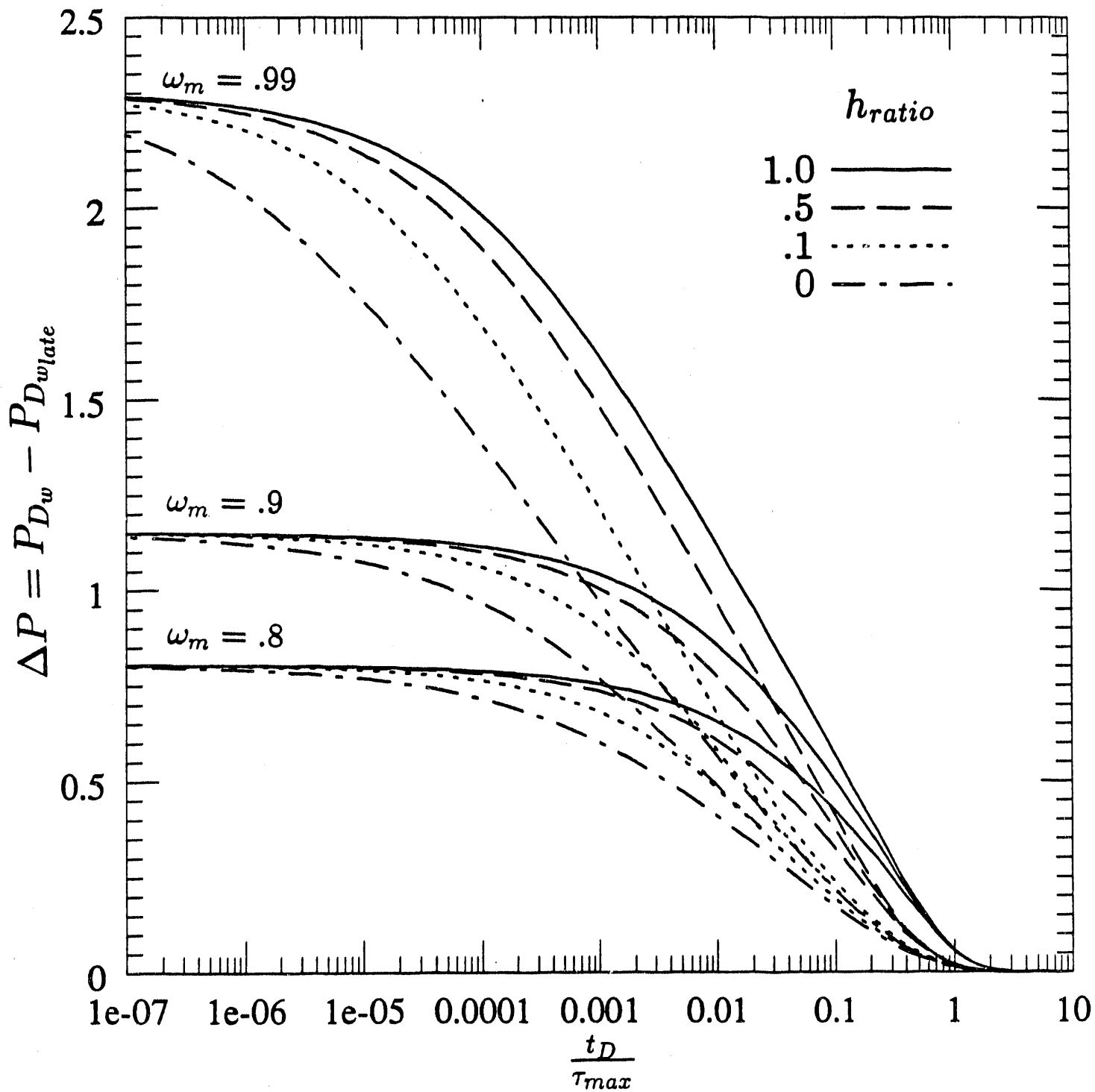
Figure 6.4: Rectangular PDF: Drawdown Type Curve for Varying h_{ratio}, λ_{min}, ω_m. Accurate for $t_D > 100$ and $\lambda_{min} < 10^{-4}$.

which is typical of the PSS response of Warren and Root. A symmetric PSS type response develops even if the no skin profile is asymmetric. As interporosity skin increases, the derivative profile shifts in time, giving apparent λ values that are too small (more dormant matrix). Thus, if interporosity skin exists, interpretation of pressure transient tests by the Warren and Root model underestimates λ and fracture intensity.
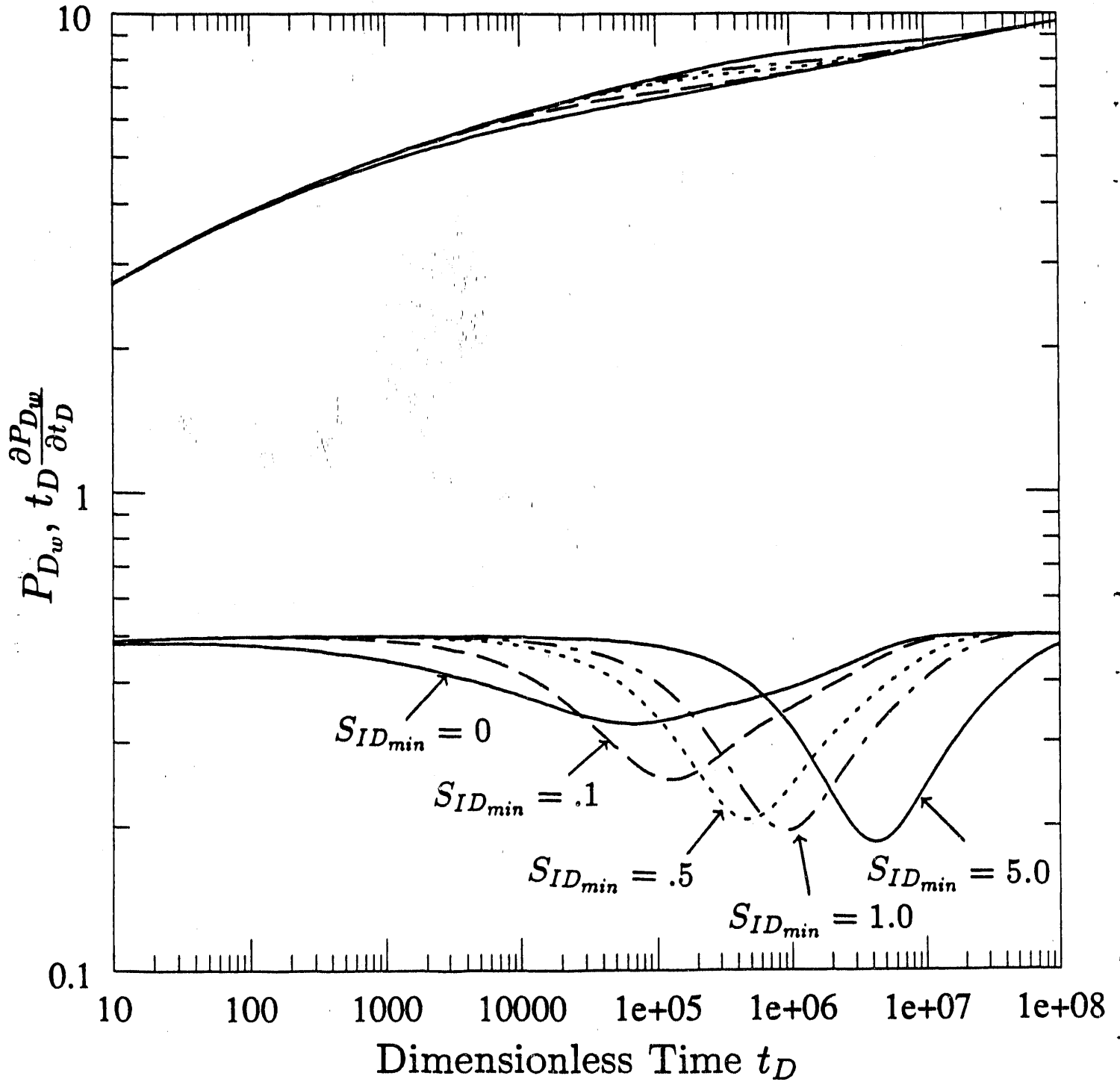
Figure 6.5: Rectangular PDF: Effect of Interporosity Skin, $h_{ratio} = .1$, $\lambda_{min} = 10^{-7}$, $\omega_m = .9$.

Section 7

Discussion-Interference Testing

Braester[11] demonstrated that drawdown (or buildup) tests in naturally fractured reservoirs may not be influenced by matrix blocks significantly away from the wellbore. Interference testing, therefore, is preferred because the response is affected by matrix blocks between the active and observation wells. A simplified solution for interference testing in the absence of storage and wellbore skin is the line source solution:

$$\overline{P}_{D_f} = \frac{K_0(r_D\sqrt{sf(s)})}{s}.$$

(7.1)

7.1   Type Curve For Interference Well Tests

For any PDF distribution, it can be shown that $\theta = \lambda_{min}r_D^2$ is a correlating parameter [20,21]. For instance, using the rectangular PDF:

$$f(sr_D^2) = \omega_f + \frac{\omega_m}{1 - h_{ratio}}\sqrt{\frac{\theta}{\omega_m sr_D^2}} \int_{h_{ratio}\sqrt{\frac{\omega_m \cdot r_D^2}{\theta}}}^{\sqrt{\frac{\omega_m \cdot r_D^2}{\theta}}} \frac{tanh(y)}{y}\,dy.$$

(7.2)

Equation 7.1 can then be evaluated using the inverse Laplace transform relation:

$$\mathcal{L}^{-1}[\overline{P}_{D_f}(sr_D^2)] = \frac{1}{r_D^2}P_{D_f}(\frac{t_D}{r_D^2}).$$

(7.3)

A type curve (Figure 7.1) is prepared using the rectangular PDF for $\omega_m = 0.9$. For each value of θ, h_{ratio} is varied from zero to one. If h_{ratio} determined from the type

30

curve is equal to one, the PDF is a Dirac delta function and the type curve is similar to that presented by Deruyck *et al* [20,21].

For large values of θ, the matrix block size variability becomes increasingly important and h_{ratio} can be better estimated. Thus, if the dimensionless distance (r_D) between the active and observation wells is large, or if λ_{min} becomes large (i.e. greater fracture intensity), then matrix block size variability becomes a key parameter in interference pressure transient analysis. Conversely, for smaller values of θ, matrix block size variability (or h_{ratio}) does not affect the pressure response significantly. Also, as θ becomes larger, the response approaches the line source solution for smaller values of $\frac{t_D}{r_D^2}$.
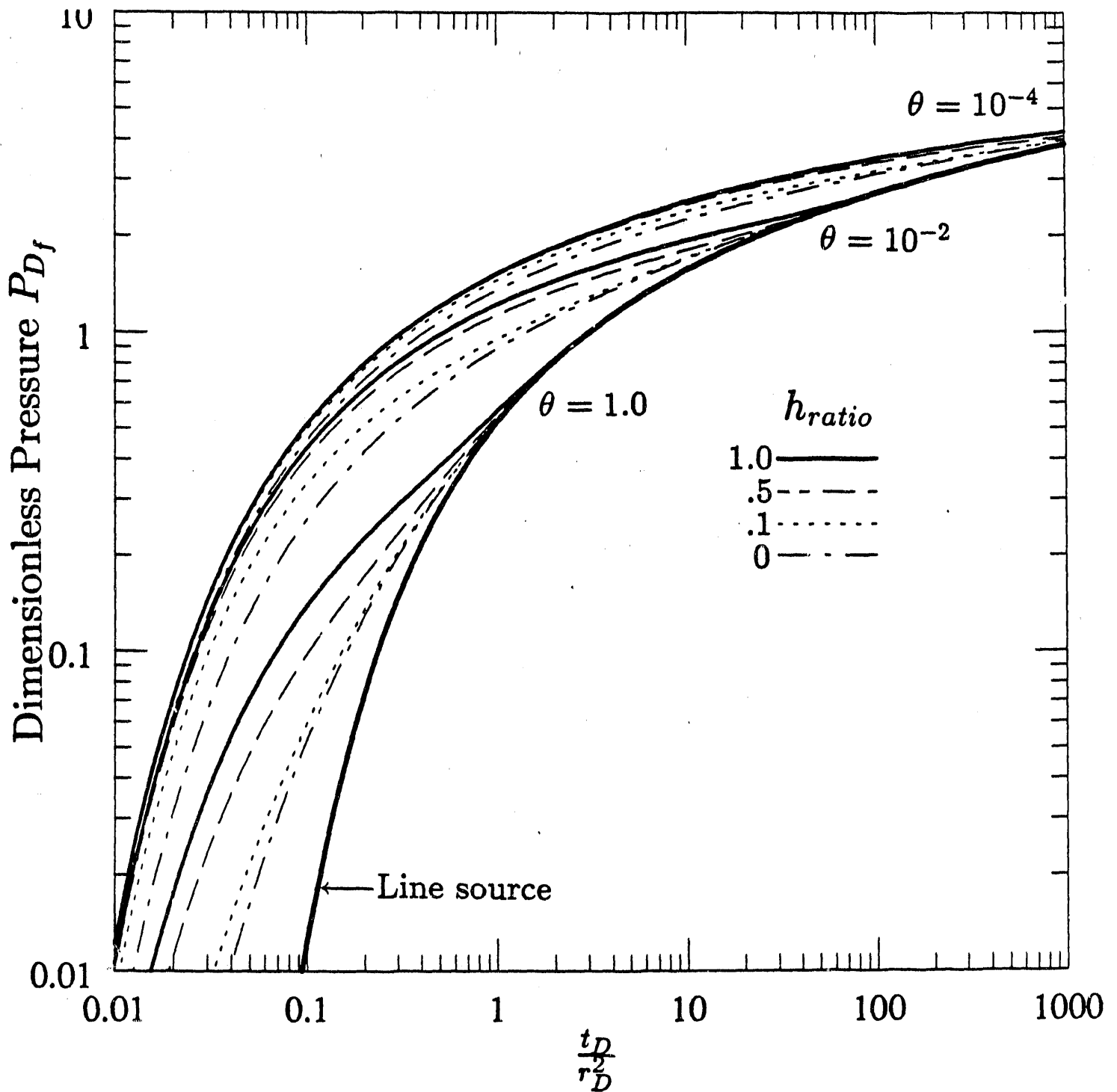
Figure 7.1: Rectangular PDF: Interference Type Curve for Varying h_{ratio}, θ, with $\omega_m = .9$.

Section 8

Conclusions

1. A formulation incorporating transient interporosity flow and interporosity skin is presented for fractured reservoirs with variable matrix block size. Exponential and linear probability density functions have been used to represent intensely and sparsely fractured reservoirs with varying degrees of fracture uniformity.

2. Type curves have been generated for drawdown and interference well tests based on the rectangular PDF and slab matrix block geometry. Type curves yield estimates of fracture intensity as well as fracture nonuniformity.

3. Fracture intensity determines the temporal position of the pressure response, while fracture uniformity affects the shape of the pressure response. For transient interporosity flow, uniformly fractured reservoirs exhibit asymmetric derivative profiles, whereas nonuniformly fractured reservoirs exhibit symmetric profiles.

4. The parameter h_{ratio} quantifies the degree of fracture uniformity. Uniform fracturing is indicated when h_{ratio} is near one, while nonuniform fracturing is indicated when h_{ratio} is near zero. For an extremely nonuniform fractured reservoir (h_{ratio} approaching zero), the pressure response is similar to a nonfractured homogeneous reservoir response.

5. Matrix block size variability (h_{ratio}) cannot be estimated in the presence of interporosity skin damage. The Warren and Root model overestimates matrix block size if interporosity skin is present.

Section 9

Nomenclature

a	= exponential PDF constant
b	= intercept of linear PDF
c_f	= fracture compressibility
c_m	= matrix compressibility
C_D	= dimensionless wellbore storage
c_t	= total compressibility
f(s)	= Laplace space function
h	= matrix block size characteristic length (Volume/Surface Area)
h_D	= dimensionless matrix block size length
h_f	= fracture thickness
h_{max}	= maximum block size length
h_{min}	= minimum block size length
h_{ratio}	= ratio of h_{min} to h_{max}
h_s	= interporosity damaged zone thickness
k_f	= fracture permeability
k_m	= matrix permeability
k_s	= interporosity damaged zone permeability
$K_0(x)$	= modified Bessel function, second kind, zero order
$K_1(x)$	= modified Bessel function, second kind, first order
m	= slope of linear PDF

P_{D_f}	= dimensionless fracture pressure
P_{D_m}	= dimensionless matrix pressure
P_{D_w}	= dimensionless wellbore pressure
P_f	= fracture fluid pressure
$P(h)$	= block size distribution function
$P(h_D)$	= dimensionless block size distribution function
P_i	= initial reservoir pressure
P_m	=' matrix fluid pressure
P_{wf}	= wellbore flowing pressure
$Q(h)$	= flow contribution from matrix size h
r	= radial coordinate
r_D	= dimensionless radial coordinate
r_w	= wellbore radius
s	= Laplace parameter
S_D	= dimensionless wellbore skin factor
S_{ID}	= dimensionless interporosity skin factor
$S_{ID_{min}}$	= minimum dimensionless interporosity skin factor
t	= time
t_D	= dimensionless time
γ	= 1.781, exponential of Euler's constant
λ	= dimensionless interporosity flow coefficient
λ_{max}	= maximum dimensionless interporosity flow coefficient
λ_{min}	= minimum dimensionless interporosity flow coefficient
τ	= dimensionless matrix response time coefficient
τ_{max}	= maximum dimensionless matrix response time coefficient
μ	= viscosity
ϵ	= coordinate normal to fracture-matrix interface
ϵ_D	= dimensionless coordinate normal to fracture-matrix interface
ϕ_f	= fracture porosity
ϕ_m	= matrix porosity
ω_f	= dimensionless fracture storativity ratio

ω_m = dimensionless matrix storativity ratio

θ = dimensionless correlation parameter

Appendix A

Derivation of General Solution

The dimensionless flow equations and boundary conditions are:

$$\frac{\partial^2 P_{D_f}}{\partial r_D^2} + \frac{1}{r_D}\frac{\partial P_{D_f}}{\partial r_D} = \omega_f \frac{\partial P_{D_f}}{\partial t_D} - \int_{h_{ratio}}^{1} \lambda \frac{\partial P_{D_m}}{\partial \epsilon_D} \mid_{\epsilon_{D \approx 0}} P(h_D)\, dh_D$$

$$\frac{\partial^2 P_{D_m}}{\partial \epsilon_D^2} = \frac{\omega_m}{\lambda}\frac{\partial P_{D_m}}{\partial t_D}.$$

- $P_{D_f} = P_{D_m} = 0$ at $t_D = 0$

- $P_{D_f} = P_{D_m} = 0$ at $r_D \to \infty$

- $C_D \frac{\partial P_{D_w}}{\partial T_D} - \frac{\partial P_{D_f}}{\partial r_D} \mid_{r_D=1} = 1$

- $P_{D_w} = [P_{D_f} - S_D \frac{\partial P_{D_f}}{\partial r_D}] \mid_{r_D=1}$

- $P_{D_f} = [P_{D_m} - S_{ID}\frac{\partial P_{D_m}}{\partial \epsilon_D}] \mid_{\epsilon_D \approx 0 \; for \; slabs}$

- $\frac{\partial P_{D_m}}{\partial \epsilon_D} \mid_{\epsilon_D \approx 1 \; for \; slabs} = 0$ at no flow boundaries

where:

$$P_{D_f} = \frac{2\pi k_f h_f (P_i - P_f)}{q\mu}$$

$$P_{D_m} = \frac{2\pi k_f h_f (P_i - P_m)}{q\mu}$$

38

$$P_{D_w} = \frac{2\pi k_f h_f (P_i - P_{wf})}{q\mu}$$

$$t_D = \frac{k_f t}{(\phi_f c_f + \phi_m c_m)\mu r_w^2}$$

$$r_D = \frac{r}{r_w}$$

$$C_D = \frac{C}{2\pi h_f c_t r_w^2}$$

$$\lambda = \frac{k_m r_w^2}{k_f h^2}$$

$$\lambda_{min} = \frac{k_m r_w^2}{k_f h_{max}^2}$$

$$\lambda_{max} = \frac{k_m r_w^2}{k_f h_{min}^2}$$

$$\omega_m = \frac{\phi_m c_m}{\phi_f c_f + \phi_m c_m}$$

$$\omega_f = 1 - \omega_m$$

$$h_D = \frac{h}{h_{max}}$$

$$\epsilon_D = \frac{\epsilon}{h}$$

$$P(h_D) = h_{max} P(h).$$

Other matrix block geometries can be included in the solution by changing the interporosity boundary conditions. After applying Laplace transforms to the flow equations and boundary conditions one obtains Equations 4.3 and 4.4.

Appendix B

Computer Programs

```
C-----------------------------------------------------------------
C----------------------EXACT EXPONENTIAL SOLUTION-----------------
C-----------------------------------------------------------------
C THIS PROGRAM CALCULATES THE EXACT SOLUTION FOR THE TRANSIENT
C INTERPOROSITY FLOW WELL TEST USING AN EXPONENTIAL PROBABILITY
C DENSITY FUNCTION. THE EXACT SOLUTION IN LAPLACE SPACE IS USED
C AND INVERTED VIA THE STEFEST ALGORITHYM. THE VARIABLES IN THE
C PROGRAM ARE:
C
C     AA----------EXPONENTIAL DECLINE FACTOR. FOR AA EQUAL TO
C                 ZERO USE THE LINEAR PDF MODEL.
C     RD----------DIMENSIONLESS DISTANCE FROM ACTIVE WELL
C     WF----------FRACTIONAL STORATIVITY OF THE FRACTURES TO THE
C                 BULK VOLUME STORATIVITY
C     WM----------FRACTIONAL STORATIVITY OF THE MATRIX TO THE
C                 BULK VOLUME STORATIVITY
C     HRATIO------THE RATIO OF THE MINIMUM TO MAXIMUM BLOCK SIZE
C     XLAMMAX-----THE MAXIMUM LAMBDA OF THE PROBABILITY DENSITY
C                 FUNCTION
C     XLAMMIN-----THE MINIMUM LAMBDA OF THE PROBABILITY DENSITY
C                 FUNCTION
C     XTAUMIN-----THE APPROXIMATE TIME WHEN THE MAXIMUM SIZE
C                 BLOCK EFFECTS THE PRESSURE TRANSIENT
C                 RESPONSE--TAU=WM/(1.781*LAMBDA)
C     XTAUMAX-----THE APPROXIMATE TIME WHEN THE MINIMUM SIZE
C                 BLOCK EFFECTS THE PRESSURE TRANSIENT
C     SD----------THE INTERPOROSITY SKIN FACTOR
C
C     TD----------DIMENSIONLESS TIME
C     PD----------DIMENSIONLESS FRACTURE PRESSURE
C     PDS---------DIMENSIONLESS SLOPE OF PD/LN(TD)
C                 IN THIS PROGRAM, THIS IS NOT OUTPUT
C     FS----------THE FUNCTION IN LAPLACE SPACE TO BE INVERTED
C
C     M,N---------INTERGERS USED IN STEFAST SUBROUTINE
C
C     PWD---------THE CALLABLE STEFAST SUBROUTINE
C
C     DQDAGS------THE CALLABLE INTEGRATION ROUTINE DESIGNED
C                 BY IMSL
C
C-----------------------------------------------------------------
C-----------------------------------------------------------------
      IMPLICIT DOUBLE PRECISION (A-H,O-Z)
      COMMON RD,WF,WM,XLAMMAX,XLAMMIN,AA,XXUP,SD
      COMMON M
      OPEN(UNIT=2,FILE='PROJ.OUT')
      REWIND(UNIT=2)
      OPEN(UNIT=3,FILE='PROJS.OUT')
      REWIND(UNIT=3)
      M=1
      N=12
      RD=1.
      PRINT *, 'EXPONENTIAL DECLINE A= '
      READ *, AA
      PRINT *, 'FRAC. SKIN= '
      READ *, SD
      PRINT *, 'LAMMIN= '
      READ *, XLAMMIN
      PRINT *, 'LAMMAX= '
      READ *, XLAMMAX
      PRINT *, 'WM= '
      READ *, WM
      WF=1.0-WM
      NNN=220
      TD=1.
```

```fortran
      WRITE (2,*) NNN
      WRITE (3,*) NNN
C CALCULATE THE PD, PDS IN REAL TIME SPACE USING
C THE STEFAST SUBROUTINE AND DQDAGS SUBROUTINE
      DO 10 I=1,NNN
            CALL PWD(TD,N,PD,PDS)
C THE SLOPE IS TD*D(PD/TD)
            PDS=TD*PDS
            WRITE (2,99) TD,PD
            WRITE (3,99) TD,PDS
 99         FORMAT (2X,2F24.9)
            TD=TD*1.1
 10   CONTINUE
      STOP
      END
C     ---------------------------------------------------------
C     THIS FUNCTION IS CALLED BY THE STEFAST SUBROUTINE AND
C     IS CONTAINS THE FUNCTION IN LAPLACE SPACE TO BE
C     INVERTED. THIS FUNCTION IS USED TO CALCULATE THE PD
C     IN REAL TIME SPACE.
C     ---------------------------------------------------------
      DOUBLE PRECISION FUNCTION PLAP(S)
      IMPLICIT DOUBLE PRECISION (A-H,O-Z)
      EXTERNAL F
      COMMON RD,WF,WM,XLAMMAX,XLAMMIN,AA,XXUP,SD
      COMMON M
      ERRREL=.0001
      ERRABS=0.0
      XTAUMIN=WM/(1.781*XLAMMAX)
      XTAUMAX=WM/(1.781*XLAMMIN)
      HRATIO=DSQRT(XLAMMIN/XLAMMAX)
      XLOW=DSQRT(WM*S/XLAMMAX)
      XUP=DSQRT(WM*S/XLAMMIN)
      XXUP=XUP
      CALL DQDAGS(F,XLOW,XUP,ERRABS,ERRREL,RESULT,ERREST)
      TERM=1/(DEXP(-AA*HRATIO)-DEXP(-AA))
      FS=WF+DSQRT(WM*XLAMMIN/S)*AA*TERM*RESULT
      XX=RD*DSQRT(S*FS)
      XXX=DSQRT(S*FS)
      A=DBSK0(XX)
      B=DBSK1(XXX)
      TOP=A
      BOT=S*XXX*B
      PLAP=TOP/BOT
      RETURN
      END
C     ---------------------------------------------------------
C     THIS FUNCTION IS CALLED BY THE STEFAST SUBROUTINE AND
C     CONTAINS THE FUNCTION IN LAPLACE SPACE TO BE INVERTED
C     THIS FUNCTION IS USED TO CALCULATE THE SLOPE OF
C     PD/LN(TD) IN REAL TIME SPACE.
C     ---------------------------------------------------------
      DOUBLE PRECISION FUNCTION PLAPS(S)
      IMPLICIT DOUBLE PRECISION (A-H,O-Z)
      EXTERNAL F
      COMMON RD,WF,WM,XLAMMAX,XLAMMIN,AA,XXUP,SD
      COMMON M
      ERRREL=.0001
      ERRABS=0.0
      XTAUMIN=WM/(1.781*XLAMMAX)
      XTAUMAX=WM/(1.781*XLAMMIN)
      HRATIO=DSQRT(XLAMMIN/XLAMMAX)
      XLOW=DSQRT(WM*S/XLAMMAX)
      XUP=DSQRT(WM*S/XLAMMIN)
      XXUP=XUP
      CALL DQDAGS(F,XLOW,XUP,ERRABS,ERRREL,RESULT,ERREST)
```

```fortran
      TERM=1/(DEXP(-AA*HRATIO)-DEXP(-AA))
      FS=WF+DSQRT(WM*XLAMMIN/S)*AA*TERM*RESULT
      XX=RD*DSQRT(S*FS)
      XXX=DSQRT(S*FS)
      A=DBSK0(XX)
      B=DBSK1(XXX)
      TOP=A
      BOT=XXX*B
      PLAPS=TOP/BOT
      RETURN
      END
C     -----------------------------------------------------------
C     THIS IS THE FUNCTION ASSOCIATED WITH THE SPECIFIED
C     PROBABILITY DENSITY FUNCTION AND IS USED AS INPUT TO
C     THE NUMERICAL INTEGRATION SUBROUTINE DQDAGS
C     -----------------------------------------------------------
      DOUBLE PRECISION FUNCTION F(X)
      COMMON RD,WF,WM,XLAMMAX,XLAMMIN,AA,XXUP,SD
      IMPLICIT DOUBLE PRECISION (A-H,O-Z)
      F=DEXP(-AA*X/XXUP)*(DTANH(X))/(X*(1+SD*XXUP*DTANH(X)))
      RETURN
      END
```

```
C------------------------------------------------------------------
C---------------------EXACT LINEAR SOLUTION------------------
C------------------------------------------------------------------
C THIS PROGRAM CALCULATES THE EXACT SOLUTION FOR THE TRANSIENT
C INTERPOROSITY FLOW WELL TEST USING A LINEAR PROBABILITY
C DENSITY FUNCTION. THE EXACT SOLUTION IN LAPLACE SPACE IS USED
C AND INVERTED VIA THE STEFEST ALGORITHYM. THE VARIABLES IN THE
C PROGRAM ARE:
C
C        XM----------SLOPE OF LINEAR PROBABILITY DENSITY FUNCTION
C        XB----------INTERCEPT OF LINEAR PROBABILITY DENSITY FUNCTION
C                    THIS IS DETERMINED BY THE PROGRAM DUE TO THE
C                    APPLICATION OF THE FACT THAT THE AREA MUST BE
C                    EQUAL TO ONE
C        RD----------DIMENSIONLESS DISTANCE FROM ACTIVE WELL
C        WF----------FRACTIONAL STORATIVITY OF THE FRACTURES TO THE
C                    BULK VOLUME STORATIVITY
C        WM----------FRACTIONAL STORATIVITY OF THE MATRIX TO THE
C                    BULK VOLUME STORATIVITY
C        HRATIO------THE RATIO OF THE MINIMUM TO MAXIMUM BLOCK SIZE
C        XLAMMAX-----THE MAXIMUM LAMBDA OF THE PROBABILITY DENSITY
C                    FUNCTION
C        XLAMMIN-----THE MINIMUM LAMBDA OF THE PROBABILITY DENSITY
C                    FUNCTION
C        XTAUMIN-----THE APPROXIMATE TIME WHEN THE MAXIMUM SIZE
C                    BLOCK EFFECTS THE PRESSURE TRANSIENT
C                    RESPONSE--TAU=WM/(1.781*LAMBDA)
C        XTAUMAX-----THE APPROXIMATE TIME WHEN THE MINIMUM SIZE
C                    BLOCK EFFECTS THE PRESSURE TRANSIENT
C        SD----------THE INTERPOROSITY SKIN FACTOR
C
C        TD----------DIMENSIONLESS TIME
C        PD----------DIMENSIONLESS FRACTURE PRESSURE
C        PDS---------DIMENSIONLESS SLOPE OF PD/LN(TD)
C                    IN THIS PROGRAM, THIS IS NOT OUTPUT
C        FS----------THE FUNCTION IN LAPLACE SPACE TO BE INVERTED
C
C        M,N---------INTERGERS USED IN STEFAST SUBROUTINE
C
C        PWD---------THE CALLABLE STEFAST SUBROUTINE
C
C        DQDAGS------THE CALLABLE INTEGRATION ROUTINE DESIGNED
C                    BY IMSL
C
C------------------------------------------------------------------------
C------------------------------------------------------------------------
C--------------------------------------------------------------
C    THIS PROGRAM CALCULATES THE LAPLACE INVERSIONS TO THE
C    DOUBLE-POROSITY MODEL.
      IMPLICIT DOUBLE PRECISION (A-H,O-Z)
      COMMON RD,WF,WM,XLAMMAX,XLAMMIN,SD,XXUP,XM,XB,HRATIO
      COMMON M
      OPEN(UNIT=2,FILE='PROJ.OUT')
      REWIND(UNIT=2)
      OPEN(UNIT=3,FILE='PROJS.OUT')
      REWIND(UNIT=3)
      M=1
      N=12
      PRINT *, 'RD= '
      READ *, RD
      PRINT *, 'FRAC. SKIN=  '
      READ *, SD
      PRINT *, 'SLOPE= '
      READ *, XM
      PRINT *, 'LAMMIN= '
      READ *, XLAMMIN
```

```fortran
      PRINT *, 'HRATIO= '
      READ *, HRATIO
      PRINT *, 'WM= '
      READ *, WM
      WF=1.0-WM
      XLAMMAX=XLAMMIN/(HRATIO**2)
      XB=(1-.5*XM+.5*XM*(HRATIO**2))/(1-HRATIO)
      FHRAT=XM*HRATIO+XB
      FONE=XM+XB
      PRINT *, 'CORR. FOR AREA ','FHRAT= ',FHRAT,'F1= ',FONE,'M= ',XM
      PRINT *, 'LAMMIN= ', XLAMMIN, 'LAMMAX= ', XLAMMAX
      NNN=220
      TD=1.
      WRITE (2,*) NNN
      WRITE (3,*) NNN
C CALCULATE THE PD, PDS IN REAL TIME SPACE USING THE
C STEFAST SUBROUTINE AND DQDAGS SUBROUTINE
      DO 10 I=1,NNN
         CALL PWD(TD,N,PD,PDS)
C THE SLOPE IS TD*D(PD/TD)
         PDS=TD*PDS
         IF(PDS.LT..0001)  PDS = .0001
         IF(PD.LT..0001)   PD = .0001
         WRITE (2,99) TD,PD
         WRITE (3,99) TD,PDS
  99     FORMAT (2X,2F24.9)
         TD=TD*1.1
  10  CONTINUE
      STOP
      END
C     -----------------------------------------------------------
C     THIS FUNCTION IS CALLED BY THE STEFAST SUBROUTINE AND
C     CONTAINS THE FUNCTION IN LAPLACE SPACE TO BE INVERTED.
C     THIS FUNCTION IS USED TO CALCULATE THE PD IN REAL
C     TIME SPACE.
C     -----------------------------------------------------------
      DOUBLE PRECISION FUNCTION PLAP(S)
      IMPLICIT DOUBLE PRECISION (A-H,O-Z)
      EXTERNAL F
      COMMON RD,WF,WM,XLAMMAX,XLAMMIN,SD,XXUP,XM,XB,HRATIO
      COMMON M
      ERRREL=.00001
      ERRABS=0.0
      XTAUMIN=WM/(1.781*XLAMMAX)
      XTAUMAX=WM/(1.781*XLAMMIN)
      HRATIO=DSQRT(XLAMMIN/XLAMMAX)
      XLOW=DSQRT(WM*S/XLAMMAX)
      XUP=DSQRT(WM*S/XLAMMIN)
      XXUP=XUP
      CALL DQDAGS(F,XLOW,XUP,ERRABS,ERRREL,RESULT,ERREST)
      FS=WF+(WM/XXUP)*RESULT
      XX=RD*DSQRT(S*FS)
      XXX=DSQRT(S*FS)
      A=DBSK0(XX)
      B=DBSK1(XXX)
      TOP=A
      BOT=S*XXX*B
      PLAP=TOP/BOT
      RETURN
      END
C     -----------------------------------------------------------
C     THIS FUNCTION IS CALLED BY THE STEFAST SUBROUTINE AND
C     CONTAINS THE FUNCTION IN LAPLACE SPACE TO BE INVERTED.
C     THIS FUNCTION IS USED TO CALCULATE THE SLOPE OF
C     PD/LN(TD) IN REAL TIME SPACE.
C     -----------------------------------------------------------
```

```fortran
      DOUBLE PRECISION FUNCTION PLAPS(S)
      IMPLICIT DOUBLE PRECISION (A-H,O-Z)
      EXTERNAL F
      COMMON RD,WF,WM,XLAMMAX,XLAMMIN,SD,XXUP,XM,XB,HRATIO
      COMMON M
      ERRREL=.0001
      ERRABS=0.0
      XTAUMIN=WM/(1.781*XLAMMAX)
      XTAUMAX=WM/(1.781*XLAMMIN)
      HRATIO=DSQRT(XLAMMIN/XLAMMAX)
      XLOW=DSQRT(WM*S/XLAMMAX)
      XUP=DSQRT(WM*S/XLAMMIN)
      XXUP=XUP
      CALL DQDAGS(F,XLOW,XUP,ERRABS,ERRREL,RESULT,ERREST)
      FS=WF+(WM/XXUP)*RESULT
      XX=RD*DSQRT(S*FS)
      XXX=DSQRT(S*FS)
      A=DBSK0(XX)
      B=DBSK1(XXX)
      TOP=A
      BOT=XXX*B
      PLAPS=TOP/BOT
      RETURN
      END
C     ------------------------------------------------------
C     THIS IS THE FUNCTION ASSOCIATED WITH THE SPECIFIED
C     PROBABILITY DENSITY FUNCTION AND IS USED AS INPUT TO
C     THE NUMERICAL INTEGRATION SUBROUTINE DQDAGS.
C     ------------------------------------------------------
      DOUBLE PRECISION FUNCTION F(X)
      IMPLICIT DOUBLE PRECISION (A-H,O-Z)
      COMMON RD,WF,WM,XLAMMAX,XLAMMIN,SD,XXUP,XM,XB,HRATIO
      F=((XM/XXUP)+XB/X)*DTANH(X)/(1+SD*XXUP*DTANH(X))
      RETURN
      END
```

```fortran
C-------------------------------------------------------------------
C     THIS PROGRAM CALCULATES THE LAPLACE INVERSIONS TO THE
C     DOUBLE-POROSITY MODEL TO CREATE A DRAWDOWN TYPE CURVE.
C     THE LATE TIME RESPONSE IS SUBTRACTED FROM PDW. THIS
C     DELTA P IS CALCULATED VS. TD/TAUMAX.
C-------------------------------------------------------------------
      IMPLICIT DOUBLE PRECISION (A-H,O-Z)
      EXTERNAL F
      COMMON RD,WF,WM,XLAMMAX,XLAMMIN,SD,XXUP,XM,XB,HRATIO
      COMMON M
      OPEN(UNIT=2,FILE='PROJ.OUT')
      REWIND(UNIT=2)
      M=1
      N=12
      PRINT *, 'RD= '
      READ *, RD
      PRINT *, 'FRAC. SKIN= '
      READ *, SD
      PRINT *, 'SLOPE= '
      READ *, XM
      PRINT *, 'HRATIO= '
      READ *, HRATIO
      PRINT *, 'LAMMIN= '
      READ *, XLAMMIN
      PRINT *, 'WM= '
      READ *, WM
      WF=1.0-WM
      XLAMMAX=XLAMMIN/(HRATIO**2)
      XB=(1-.5*XM+.5*XM*(HRATIO**2))/(1-HRATIO)
      FHRAT=XM*HRATIO+XB
      FONE=XM+XB
      PRINT *, 'LAMMIN= ', XLAMMIN,'LAMMAX= ',XLAMMAX
      PRINT *, 'FHRAT= ',FHRAT,'F1= ',FONE,'M= ',XM
      XTAUMIN=WM/(1.781*XLAMMAX)
      XTAUMAX=WM/(1.781*XLAMMIN)
      PRINT *, 'TAUMAX= ',XTAUMAX
      NNN=280
      TD=1.
      WRITE (2,*) NNN
      DO 10 I=1,NNN
         CALL PWD(TD,N,PD,PDS)
         PD=PD-.5*(DLOG(TD/(RD**2))+.80907)
         TDTAU=TD/XTAUMAX
         IF(PD.LT..0001)  PD = .0001
         IF(TDTAU.LT.1E-9) TDTAU=1E-9
         WRITE (2,99) TDTAU,PD
99       FORMAT (2X,2F24.9)
         TD=TD*1.1
10    CONTINUE
      STOP
      END
C     ----------------------------------------------------------
      DOUBLE PRECISION FUNCTION PLAP(S)
      IMPLICIT DOUBLE PRECISION (A-H,O-Z)
      EXTERNAL F
      COMMON RD,WF,WM,XLAMMAX,XLAMMIN,SD,XXUP,XM,XB,HRATIO
      COMMON M
      ERRREL=.00001
      ERRABS=0.0
      XLOW=HRATIO*DSQRT(WM*S/XLAMMIN)
      XUP=DSQRT(WM*S/XLAMMIN)
      XXUP=XUP
      CALL DQDAGS(F,XLOW,XUP,ERRABS,ERRREL,RESULT,ERREST)
      FS=WF+(WM/XXUP)*RESULT
      XX=RD*DSQRT(S*FS)
      XXX=DSQRT(S*FS)
```

```
      A=DBSK0(XX)
      B=DBSK1(XXX)
      TOP=A
      BOT=S*XXX*B
      PLAP=TOP/BOT
      RETURN
      END
C     -----------------------------------------------------
      DOUBLE PRECISION FUNCTION F(X)
      IMPLICIT DOUBLE PRECISION (A-H,O-Z)
      COMMON RD,WF,WM,XLAMMAX,XLAMMIN,SD,XXUP,XM,XB,HRATIO
      F=((XM/XXUP)+XB/X)*DTANH(X)/(1+SD*XXUP*DTANH(X))
      RETURN
      END
```

```
C------------------------------------------------------------------
C---------------------EXACT LINEAR SOLUTION-----------------------
C------------------FOR INTERFERENCE WELL TESTS-------------------
C------------------------------------------------------------------
C THIS PROGRAM CALCULATES THE EXACT SOLUTION FOR THE TRANSIENT
C INTERPOROSITY FLOW INTERFERENCE WELL TEST USING A LINEAR
C PROBABILITY DENSITY FUNCTION. THE EXACT SOLUTION IN LAPLACE
C SPACE IS USED AND INVERTED VIA THE STEFEST ALGORITHYM. THE
C PROGRAM DOES ASSUME THE FORM OF THE LINE SOURCE SOLUTION IS VALID.
C THE
C VARIABLES IN THE PROGRAM ARE:
C
C      XM----------SLOPE OF T'    'NEAR PROBABILITY DENSITY
C                  FUNCTION
C      XB----------INTERCEPT OF THE LINEAR PROBABILITY DENSITY
C                  FUNCTION. THIS IS CALCULATED BY THE PROGRAM
C                  AND IT DETERMINED FROM THE FACT THAT THE
C                  AREA OF A PROBABILITY DENSITY FUNCTION MUST
C                  BE EQUAL TO ONE.
C      RD----------DIMENSIONLESS DISTANCE FROM ACTIVE WELL
C      WF----------FRACTIONAL STORATIVITY OF THE FRACTURES TO THE
C                  BULK VOLUME STORATIVITY
C      WM----------FRACTIONAL STORATIVITY OF THE MATRIX TO THE
C                  BULK VOLUME STORATIVITY
C      HRATIO------THE RATIO OF THE MINIMUM TO MAXIMUM BLOCK SIZE
C      XLAMMAX-----THE MAXIMUM LAMBDA OF THE PROBABILITY DENSITY
C                  FUNCTION
C      XLAMMIN-----THE MINIMUM LAMBDA OF THE PROBABILITY DENSITY
C                  FUNCTION
C      XTAUMIN-----THE APPROXIMATE TIME WHEN THE MAXIMUM SIZE
C                  BLOCK EFFECTS THE PRESSURE TRANSIENT
C                  RESPONSE--TAU=WM/(1.781*LAMBDA)
C      XTAUMAX-----THE APPROXIMATE TIME WHEN THE MINIMUM SIZE
C                  BLOCK EFFECTS THE PRESSURE TRANSIENT
C      THETA-------CORRELATION PARAMETER (THETA=LAMBDA*RD**2)
C      SD----------THE INTERPOROSITY SKIN FACTOR
C
C      TD----------DIMENSIONLESS TIME
C      TDRD--------DIMENSIONLESS TIME, INCLUDES RD**2 TERM
C                  (I.E. TDRD=TD/RD**2)
C      PD----------DIMENSIONLESS FRACTURE PRESSURE
C      PDS---------DIMENSIONLESS SLOPE OF PD/LN(TD)
C                  IN THIS PROGRAM, THIS IS NOT OUTPUT
C      FS----------THE FUNCTION IN LAPLACE SPACE TO BE INVERTED
C
C      M,N---------INTERGERS USED IN STEFAST SUBROUTINE
C
C      PWD---------THE CALLABLE STEFAST SUBROUTINE
C
C      DQDAGS------THE CALLABLE INTEGRATION ROUTINE DESIGNED
C                  BY IMSL
C
C------------------------------------------------------------------
C------------------------------------------------------------------
C------------------------------------------------------------------
      IMPLICIT DOUBLE PRECISION (A-H,O-Z)
      COMMON RD,WF,WM,XLAMMAX,XLAMMIN,SD,XXUP,XM,XB,HRATIO
      COMMON M
      OPEN(UNIT=2,FILE='PROJ.OUT')
      REWIND(UNIT=2)
      OPEN(UNIT=3,FILE='PROJS.OUT')
      REWIND(UNIT=3)
      M=1
      N=12
      PRINT *, 'FRAC. SKIN= '
      READ *, SD
```

```
      PRINT *, 'RD= '
      READ *, RD
      PRINT *, 'SLOPE= '
      READ *, XM
      PRINT *, 'THETA= '
      READ *, THETA
      PRINT *, 'HRATIO= '
      READ *, HRATIO
      PRINT *, 'WM= '
      READ *, WM
      WF=1.0-WM
      XLAMMIN=THETA/(RD**2)
      XLAMMAX=XLAMMIN/(HRATIO**2)
      PRINT *, 'LAMMIN= ',XLAMMIN,'LAMMAX= ',XLAMMAX
      XB=(1-.5*XM+.5*XM*(HRATIO**2))/(1-HRATIO)
      FHRAT=XM*HRATIO+XB
      FONE=XM+XB
      PRINT *, 'CORR. FOR AREA ','FHRAT= ',FHRAT,'F1= ',FONE,'M= ',XM
      NNN=220
      TD=1.
      WRITE (2,*) NNN
      WRITE (3,*) NNN
C CALCULATE THE PD, PDS IN REAL TIME SPACE USING THE
C STEFAST SUBROUTINE AND DQDAGS SUBROUTINE.
      DO 10 I=1,NNN
          CALL PWD(TD,N,PD,PDS)
C THE SLOPE IS TD*D(PD/TD)
          PDS=TD*PDS
          IF(PDS.LT..0001)  PDS = .0001
          IF(PD.LT..0001)   PD = .0001
          IF(TD.LT.1E-9) TD=1E-9
          TDRD=TD/(RD**2)
          WRITE (2,99) TDRD,PD
          WRITE (3,99) TDRD,PDS
99        FORMAT (2X,2F24.9)
          TD=TD*1.1
10    CONTINUE
      STOP
      END
C     --------------------------------------------------------
C
C     THIS FUNCTION IS CALLED BY THE STEFAST SUBROUTINE AND
C     CONTAINS THE FUNCTION IN LAPLACE SPACE TO BE INVERTED.
C     THIS FUNCTION IS USED TO CALCULATE THE PD IN REAL TIME
C     SPACE.
C     --------------------------------------------------------
      DOUBLE PRECISION FUNCTION PLAP(S)
      IMPLICIT DOUBLE PRECISION (A-H,O-Z)
      EXTERNAL F
      COMMON RD,WF,WM,XLAMMAX,XLAMMIN,SD,XXUP,XM,XB,HRATIO
      COMMON M
      ERRREL=.00001
      ERRABS=0.0
      XTAUMIN=WM/(1.781*XLAMMAX)
      XTAUMAX=WM/(1.781*XLAMMIN)
      XUP=DSQRT(WM*S/XLAMMIN)
      XLOW=HRATIO*XUP
      XXUP=XUP
      CALL DQDAGS(F,XLOW,XUP,ERRABS,ERRREL,RESULT,ERREST)
      FS=WF+(WM/XXUP)*RESULT
      XX=RD*DSQRT(S*FS)
      XXX=DSQRT(S*FS)
      A=DBSK0(XX)
      B=DBSK1(XXX)
      TOP=A
      BOT=S*XXX*B
      PLAP=TOP/BOT
```

```
      RETURN
      END
C     -------------------------------------------------------------
C     THIS FUNCTION IS CALLED BY THE STEFAST SUBROUTINE AND
C     CONTAINS THE FUNCTION IN LAPLACE SPACE TO BE INVERTED
C     THIS FUNCTION IS USED TO CALCULATE THE SLOPE OF
C     PD/LN(TD)  IN REAL TIME SPACE.
C     -------------------------------------------------------------
      DOUBLE PRECISION FUNCTION PLAPS(S)
      IMPLICIT DOUBLE PRECISION (A-H,O-Z)
      EXTERNAL F
      COMMON RD,WF,WM,XLAMMAX,XLAMMIN,SD,XXUP,XM,XB,HRATIO
      COMMON M
      ERRREL=.0001
      ERRABS=0.0
      XTAUMIN=WM/(1.781*XLAMMAX)
      XTAUMAX=WM/(1.781*XLAMMIN)
      XUP=DSQRT(WM*S/XLAMMIN)
      XLOW=HRATIO*XUP
      XXUP=XUP
      CALL DQDAGS(F,XLOW,XUP,ERRABS,ERRREL,RESULT,ERREST)
      FS=WF+(WM/XXUP)*RESULT
      XX=RD*DSQRT(S*FS)
      XXX=DSQRT(S*FS)
      A=DBSK0(XX)
      B=DBSK1(XXX)
      TOP=A
      BOT=XXX*B
      PLAPS=TOP/BOT
      RETURN
      END
C     -------------------------------------------------------------
C     THIS IS THE FUNCTION ASSOCIATED WITH THE SPECIFIED
C     PROBABILITY DENSITY FUNCTION AND IS USED AS INPUT TO
C     THE NUMERICAL INTEGRATION SUBROUTINE DQDAGS.
C     -------------------------------------------------------------
      DOUBLE PRECISION FUNCTION F(X)
      IMPLICIT DOUBLE PRECISION (A-H,O-Z)
      COMMON RD,WF,WM,XLAMMAX,XLAMMIN,SD,XXUP,XM,XB,HRATIO
      F=((XM/XXUP)+XB/X)*DTANH(X)/(1+SD*XXUP*DTANH(X))
      RETURN
      END
```

```
C                    THE STEHFEST ALGORITHM
C                    ****************************
C
      SUBROUTINE PWD(TD,N,PD,PDS)
C         THIS FUNTION COMPUTES NUMERICALLY THE LAPLACE TRNSFORM
C         INVERSE OF F(S).
      IMPLICIT DOUBLE PRECISION (A-H,O-Z)
      DIMENSION G(50),V(50),H(25)
      COMMON RD,WF,WM,XLAMMAX,XLAMMIN,AA,XXUP,SD
      COMMON M
C
C         NOW IF THE ARRAY V(I) WAS COMPUTED BEFORE THE PROGRAM
C         GOES DIRECTLY TO THE END OF THE SUBRUTINE TO CALCULATE
C         F(S).
      IF (N.EQ.M) GO TO 17
      M=N
      DLOGTW=0.6931471805599
      NH=N/2
C
C         THE FACTORIALS OF 1 TO N ARE CALCULATED INTO ARRAY G.
      G(1)=1
      DO 1 I=2,N
         G(I)=G(I-1)*I
1     CONTINUE
C
C         TERMS WITH K ONLY ARE CALCULATED INTO ARRAY H.
      H(1)=2./G(NH-1)
      DO 6 I=2,NH
         FI=I
         IF(I-NH) 4,5,6
4        H(I)=FI**NH*G(2*I)/(G(NH-I)*G(I)*G(I-1))
         GO TO 6
5        H(I)=FI**NH*G(2*I)/(G(I)*G(I-1))
6     CONTINUE
C
C         THE TERMS (-1)**NH+1 ARE CALCULATED.
C         FIRST THE TERM FOR I=1
      SN=2*(NH-NH/2*2)-1
C
C         THE REST OF THE SN'S ARECALCULATED IN THE MAIN RUTINE.
C
C
C         THE ARRAY V(I) IS CALCULATED.
      DO 7 I=1,N
C
C         FIRST SET V(I)=0
         V(I)=0.
C
C         THE LIMITS FOR K ARE ESTABLISHED.
C         THE LOWER LIMIT IS K1=INTEG((I+1/2))
         K1=(I+1)/2
C
C         THE UPPER LIMIT IS K2=MIN(I,N/2)
         K2=I
         IF (K2-NH) 8,8,9
9        K2=NH
C
C         THE SUMMATION TERM IN V(I) IS CALCULATED.
8        DO 10 K=K1,K2
            IF (2*K-I) 12,13,12
12          IF (I-K) 11,14,11
11          V(I)=V(I)+H(K)/(G(I-K)*G(2*K-I))
            GO TO 10
13          V(I)=V(I)+H(K)/G(I-K)
            GO TO 10
14          V(I)=V(I)+H(K)/G(2*K-I)
```

```
10        CONTINUE
C
C           THE V(I) ARRAY IS FINALLY CALCULATED BY WEIGHTING
C           ACCORDING TO SN.
          V(I)=SN*V(I)
C
C           THE TERM SN CHANGES ITS SIGN EACH ITERATION.
          SN=-SN
7         CONTINUE
C
C           THE NUMERICAL APPROXIMATION IS CALCULATED.
17        A=DLOGTW/TD
          PD=0
          PDS=0
          DO 15 I=1,N
            ARG=A*I
            PD=PD+V(I)*PLAP(ARG)
            PDS=PDS+V(I)*PLAPS(ARG)
15        CONTINUE
          PD=PD*A
          PDS=PDS*A
18        RETURN
          END
```

Bibliography

[1] Aguilera, R.:, "Discussion of New Pressure Transient Analysis Methods for Naturally Fractured Reservoirs", J. Pet. Tech., 849–851, (May 1984).

[2] Aguilera, R.:, Naturally Fractured Reservoirs, Petroleum Publishing Co. Tulsa, OK, (1980).

[3] Aydin, A.:, Faulting in Sandstone, PhD thesis, Stanford Univ., (Nov. 1977).

[4] Barenblatt, et al.:, "Basic Concepts in the Theory of Homogeneous Liquids in Fissured Rocks", J. Appl. Math. Mech., 24:1286–1303, (1960).

[5] Barenblatt, G.E.:, "On Certain Boundary-Value Problems for the Equations of Seepage of a Liquid in Fissured Rocks", J. Appl. Math. Mech., 27:513–518, (1963).

[6] Barker, J.A.:, "Block-Geometry Functions Characterizing Transport in Densely Fissured Media", J. Hydrology, 77:263–279, (1985).

[7] Belani, A.K. and Jalali-Yazdi, Y.:, "Estimation of Matrix Block Size Distribution in Naturally Fractured Reservoirs", SPE 18171, presented at the 63rd Fall Technical Conference held in, Houston, TX, Oct., 1988.

[8] Benson, S.M. and Lai, C.H.:, "Analysis of Interference Data in a Highly Heterogeneous Naturally Fractured Geothermal Reservoir", SPE 13252, presented at the 59th Fall Technical Conference held in, Houston, TX, Sept., 1984.

[9] Bles, J.L. and Feuga, B.:, The Fracture of Rocks, North Oxford Academic Publishers, (1986).

[10] Bourdet, D. and Gringarten, A.C.:, *"Determination of Fissured Volume and Block Size in Fractured Reservoirs by Type-Curve Analysis"*, SPE 9293, presented at the 55th Fall Technical Conference held in, Dallas, Texas, Sept., 1980.

[11] Braester, C.:, *"Influence of Block Size on the Transition Curve for a Drawdown Test in a Naturally Fractured Reservoir"*, Soc. Pet. Eng. J., 498–504, (1984).

[12] Chih-Cheng Chen, et al.:, *"Pressure Response at Observation Wells in Fractured Reservoir"*, SPE 10839, presented at the SPE/DOE Unconventional Gas Recovery Symposium held in, Pittsburgh, Pa., May, 1982.

[13] Cinco-Ley, H. and Samaniego, V.:, *"Pressure Transient Analysis for Naturally Fractured Reservoirs"*, SPE 11026, presented at the 57th Annual Fall Technical Conference held in, New Orleans, LA, Sept., 1982.

[14] Cinco-Ley, H., et al.:, *"The Pressure Transient Behavior for Naturally Fractured Reservoirs with Multiple Block Size"*, SPE 14168, presented at the 60th Fall Technical Conference held in, Las Vegas, NV, Sept., 1985.

[15] Geothermal Resources Council:, *"Fractures in Geothermal Reservoirs"*, presented at Geothermal Workshop in Honolulu, HA, (August 1982).

[16] Crawford, G.E., et al.:, *"Analysis of Pressure Buildup Tests in Naturally Fractured Reservoirs"*, J. Pet. Tech., 1295–1300, (Nov. 1976).

[17] de Swaan, O.A.:, *"Analytical Solutions for Determining Naturally Fractured Reservoir Properties by Well Testing"*, Soc. Pet. Eng. J., (June 1976).

[18] de Swaan, O.A.:, *"Influence of Shape and Skin of Matrix-Rock Blocks on Pressure Transients in Fractured Reservoirs"*, SPE 15637, presented at the 61st Fall Technical Conference held in, New Orleans, LA, Oct., 1986.

[19] de Swaan, O.A.:, *"Pressure Tests in Naturally Fractured Reservoirs"*, Rev. Inst. Mex. Petrol, 16(4):36–60, (Oct. 1984).

[20] Deruyck, B.G.:, *Interference Well Test Analysis For A Naturally Fractured Reservoir*, Master's thesis, Stanford Univ., (June 1980).

[21] Deruyck, B.G., et al.:, *"Interpretation of Interference Tests in Reservoirs with Double Porosity Behavior-Theory and Field Examples"*, SPE 11025, presented at the 57th Fall Technical Conference held in, New Orleans, LA, Sept., 1982.

[22] Dyer, J.R.:, *Jointing in Sandstones, Arches National Park, Utah*, PhD thesis, Stanford Univ., (August 1983).

[23] Gringarten, A.C.:, *"Interpretation of Tests in Fissured and Multilayered Reservoirs With Double-Porosity Behavior: Theory and Practice"*, J. Pet. Tech., 549-564, (April 1984).

[24] Gringarten, A.C.:, *"Interpretation of Tests in Fissured Reservoirs and Multilayered Reservoirs with Double Porosity Behavior"*, SPE 10044, presented at the Internation Petroleum Symposium held in, Beijing, China, March, 1982.

[25] Isaacs, C.M.:, *"Geology and Physical Properties of the Monterey Formation, California"*, SPE 12733, presented at the California Regional Meeting held in, Long Beach, April, 1984.

[26] Jalali-Yazdi, Y.:, *Pressure Transient Behavior of Heterogeneous Naturally Fractured Reservoirs*, PhD thesis, Univ. of Southern California, (Sept. 1987).

[27] Jalali-Yazdi, Y. and Ershaghi, I.:, *"Pressure Transient Analysis of Heterogeneous Naturally Fractured Reservoirs"*, SPE 16341, presented at the California Regional Meeting held in, Ventura, CA, April, 1987.

[28] Jalali-Yazdi, Y. and Ershaghi, I.:, *"A Unified Type Curve Approach for Pressure Transient Analysis of Naturally Fractured Reservoirs"*, SPE 16778, presented at the 62nd Fall Technical Conference held in, Dallas, TX, Sept, 1987.

[29] Johns, R.T.:, *Comparison of Pressure Transient Response in Intensely and Sparsely Fractured Reservoirs*, Master's thesis, Stanford Univ., (1989).

[30] Johns, R.T. and Jalali-Yazdi, Y.:, *"Comparison of Pressure Transient Response in Intensely and Sparsely Fractured Reservoirs"*, SPE 18800, presented at the Calif. Reg. Mtg. held in, Bakersfield, CA, April, 1989.

[31] Kazemi, H.:, *"Pressure Transient Analysis of Naturally Fractured Reservoirs with Uniform Fracture Distribution"*, Soc. Pet. Eng. J., 451–62, (Dec. 1969).

[32] Kazemi, H., et al.:, *"The Interpretation of Interference Tests in Naturally Fractured Reservoirs with Uniform Fracture Distribution"*, Soc. Pet. Eng., 463–472, (Dec. 1969).

[33] Kucuk, F. and Sawyer, W.K.:, *"Transient Flow In Naturally Fractured Reservoirs and Its Application to Devonian Gas Shales*, SPE 9397, presented at the 55th Fall Technical Conference held in, Dallas, TX, Sept., 1980.

[34] Mattax, C.C. and Kyte, J.R.:, *"Imbibition Oil Recovery from Fractured, Water-Drive Reservoir"*, Soc. Pet. Eng., 177–184, (June 1962).

[35] Mavor, M.L. and Cinco-Ley, H.:, *"Transient Pressure Behavior of Naturally Fractured Reservoirs"*, SPE 7977, presented at the California Regional Meeting held in, Ventura, CA, April, 1979.

[36] McQuillan, H.:, *"Fracture Patterns on Kuh-e Asmari Anticline, Southwest Iran"*, AAPG Bulletin, 58(2):236–246, (Feb. 1974).

[37] McQuillan, H.:, *"Small Scale Fracture Density in Asmari Formation of Southwest Iran and its Relation to Bed Thickness"*, AAPG Bulletin, 57(12):2367–2385, (Dec. 1973).

[38] Moench, A.F.:, *"Double-Porosity Models for a Fissured Groundwater Reservoir with Fracture Skin"*, J. Water Resources, 20(7):831–846, (July 1984).

[39] Najurieta, H.L.:, *"Interference and Pulse Testing in Uniformly Fractured Reservoirs"*, SPE 8283, presented at the 54th Fall Technical Conference held in, Las Vegas, NV, Sept., 1979.

[40] Najurieta, H.L.:, *"A Theory for Pressure Transient Analysis in Naturally Fractured Reservoirs"*, *J. Pet. Tech.*, 1241–1250, (July 1980).

[41] Odeh, A.S.:, *"Unsteady-State Behavior of Naturally Fractured Reservoirs"*, *Soc. Pet Eng. J.*, 60–66, (March 1965).

[42] Ogbe, D.O.:, *Pulse Testing in the Presence of Wellbore Storage and Skin Effects*, PhD thesis, Stanford Univ., (Jan. 1984).

[43] Pollard, D.D. and Aydin, A.:, *"Progress in Understanding Jointing Over the Past Century"*, *Geol. Soc. Amer. Bull.-Centennial Vol.*, (March 1988).

[44] Reiss, L.H.:, *The Reservoir Engineering Aspects of Fractured Formations*, Gulf Publishing Co., (1980).

[45] Schapery, A.:, *Approximate Methods of Transform Inversion for Viscoelastic Stress Analysis*, Technical Report, 4th U.S. National Congress Appl. Math., (1961).

[46] Segall, P.:, *The Development of Joints and Faults*, PhD thesis, Stanford Univ., (July 1981).

[47] Serra, K.V., Reynolds, A.C., and Raghavan, R.:, *"New Pressure Transient Analysis Methods for Naturally Fractured Reservoirs"*, SPE 10780, presented at the California Regional Meeting held in, San Francisco, CA, March, 1982.

[48] Stehfest, H.:, *"Numerical Inversion of Laplace Transforms"*, *J. ACM*, 13(1):47–49, (Jan. 1970).

[49] Streltsova, T.D.:, *"Hydrodynamics of Groundwater Flow in a Fractured Formation"*, *J. Water Resources*, 3(12):405–414, (1976).

[50] Streltsova, T.D.:, *"Well Pressure Behavior of a Naturally Fractured Reservoir"*, SPE 10782, presented at the California Regional Meeting held in, San Francisco, CA, March, 1982.

[51] Uldricht, D.O. and Ershaghi, I.:, *"A Method for Estimating the Interporosity Flow Parameter in Naturally Fractured Reservoirs"*, SPE 7142, presented at the California Regional Meeting held in, San Francisco, CA, April, 1978.

[52] Warren, J.E. and Root, P.J.:, *"The Behavior of Naturally Fractured Reservoirs"*, *Soc. Pet. Eng. J.*, 245–55, (Sept. 1963).

[53] Williamson, J.W.:, *The Effect of Wellbore Storage and Damage at the Producing Well on Interference Test Analysis*, Master's thesis, Stanford Univ., (June 1977).

DATE
FILMED
7/127/192